



ORIGINAL ARTICLE

Cytoprotective organoselenium compounds for oligodendrocytes



Saad Shaaban^{a,b,*}, Amira Zarrouk^{c,d}, Dominique Vervandier-Fasseur^e,
Yasair S.Al-Faiyz^a, Hany El-Sawy^{a,f}, Ismail Althagafi^g, Pierre Andreolletti^c,
Mustapha Cherkaoui-Malki^{c,**}

^a Department of Chemistry, College of Science, King Faisal University, P.O. Box 380, Al-Ahsa 31982, Saudi Arabia

^b Organic Chemistry Division, Department of Chemistry, Faculty of Science, Mansoura University, Egypt

^c Univ. Bourgogne-Franche Comté, Laboratoire BioPeroxIL (Biochimie du Peroxysome, Inflammation et Métabolisme Lipidique), Dijon, France

^d Faculté de Médecine, Laboratoire de Nutrition-Aliments Fonctionnels et Santé Vasculaire (LR12ES05), Monastir & Faculté de Médecine, Université de Monastir, Sousse, Tunisia

^e Institut de Chimie Moléculaire de l'Université de Bourgogne, UMR6302, CNRS, Université Bourgogne Franche-Comté, Dijon, France

^f Biochemistry division, Department of Chemistry, Faculty of Science, Tanta University, Tanta, Egypt

^g Chemistry Department, Faculty of Applied Science, Umm Al-Qura University, Makkah, Saudi Arabia

Received 27 November 2020; accepted 28 January 2021

Available online 3 February 2021

KEYWORDS

Organoselenium;
Ugi reaction;
Tetrazole;
Antioxidant;
Oligodendrocytes;
Cytoprotective

Abstract Herein we report the synthesis of peptide-like and tetrazole-based organoselenium compounds via Ugi and Ugi-azide reactions, respectively. The organoselenium compounds' intrinsic cytoprotective and antioxidant capacities were evaluated in 158 N and 158JP murine oligodendrocytes. Furthermore, their redox properties were theoretically evaluated using Molecular Operating Environment-docking studies. Most of the compounds did not exhibit any cytotoxicity against the 158JP and 158 N cells. Among the tested compounds, the tetrazole- (e.g., **6**, **7**, and **9**) and the pseudo-peptide-based organoselenium compounds (e.g., **11**, **15**, and **17**) displayed antioxidant properties. On the other hand, the quinones- (e.g., **4c** and **18**) and the pseudo-peptides-based (e.g., **12**, **14**, and **17**) organoselenium compounds exhibited prooxidant activities. Furthermore, the tetrazole-

* Corresponding author at: Department of Chemistry, College of Science, King Faisal University, P.O. Box 380 Al-Ahsa, 31982, Saudi Arabia.

** Corresponding author at: Laboratoire BioPeroxIL EA7270, Univ. Bourgogne-Franche Comté, Faculté des Sciences Gabriel, 6 Bd Gabriel, 21000 Dijon, France.

E-mail addresses: sbrahim@kfu.edu.sa, dr_saad_chem@mans.edu.eg (S. Shaaban), malki@u-bourgogne.fr (M. Cherkaoui-Malki).

Peer review under responsibility of King Saud University.



based organoselenium compounds **5** and **9** and the selenopeptide **11** and **15** showed good GPx-like activity. Some of the newly synthesized organoselenium compounds presented interesting antioxidant and cytoprotective activities and are therefore considered potential myelin diseases drug candidates.

© 2021 The Authors. Published by Elsevier B.V. on behalf of King Saud University. This is an open access article under the CC BY-NC-ND license (<http://creativecommons.org/licenses/by-nc-nd/4.0/>).

1. Introduction

Myelin sheath plays a pivotal role in the survival and transmission of neuron signals (Liu and Zhou, 2013; Hughes and Appel, 2019). It's mainly formed from oligodendrocyte (OL) cell membranes wrapped around the neuron's axons in a spiral and multilayered fashion (Bechler and Byrne, 2015). Thus, OLs are crucial for neurons' long-term integrity via their axons' myelination (El Waly et al., 2014). Oxidative stress (OS) is a crucial mediator in OL dysfunction by demyelination and disruption of normal axonal function and the dysfunction of mitochondria and peroxisomes (Coman et al., 2005; Vanzulli et al., 2020). The latter are common features in several neurodegenerative disorders such as Alzheimer's and Parkinson's diseases (Ransohoff, 2016). Oxidative damage usually occurs when the endogenous reactive oxygen species (a.k.a. ROS) production overwhelms the human body's antioxidant capacity (El Waly et al., 2014; Mahalingaiah and Singh, 2014; Karihtala et al., 2012). Antioxidants, therefore, maintain proper physiological function (e.g., immune defense, cell signaling, and cell death) and regulate ROS levels either via enzymatic defense systems (e.g., catalase, superoxide dismutase (SOD), glutathione peroxidase (GPx), and thioredoxin reductase (TrxR), and) or non-enzymatically (glutathione, phytochemicals, mineral, and vitamins) (Ibrahim et al., 2015; Pisoschi and Pop, 2015; Meriane et al., 2014). Thus, the development of antioxidants able to counteract the progression of OS-related illness is highly important in disease chemoprevention. Accordingly, drug development strategies are currently focusing on the development of "redox modulators" as chemopreventive agents for the redox linked diseases (Correa et al., 2000; Pons et al., 2020). Compounds that mimic the GPx selenocysteine-based mammalian enzyme are of longstanding concern as potential redox-based drugs (Ibrahim et al., 2015; Haselton et al., 2015; Luo et al., 2014). The latter protects bio-membranes and other cellular compartments from oxidative damage via detoxification/reduction of various deleterious hydroperoxides and peroxynitrite (e.g., hydrogen peroxide and lipid peroxides) using GSH as the reducing co-substrate (Parnham and Sies, 2013; Krehl et al., 2012; Nascimento et al., 2012).

Mounting evidence has shown that organoselenium agents are good GPx mimics with interesting antioxidants activity (Barbosa et al., 2017). These compounds are chemically and metabolically stable, and this increased the concern in the rational design of novel organoselenium agents (Mugesh et al., 2001; Bhabak and Mugesh, 2010). The latter was confirmed by animal model and intervention studies and pre-clinical trials (e.g., NPC, SELEBLAT, and SELECT) (Moyad, 2020). Subsequently, this fact served as an impetus for the rational design of organic selenide-based chemoprotective

and antioxidant agents (Álvarez-Pérez et al., 2018; Ali et al., 2018).

In this respect, the ebselen **I** synthetic organoselenium drug has shown interesting thioredoxin reductase- and glutathione peroxidase-like activities as well as promising neuroprotective properties (Luo et al., 2014; Parnham and Sies, 2013; Yamaguchi et al., 1998) (Fig. 1). Diphenyl diselenide **II** also has well-established antioxidant properties and GPx-like activity as well as cytoprotective properties in a variety of oxidatively stressed animal models (Ibrahim et al., 2015; Dias et al., 2014; Glaser et al., 2014; Giordani et al., 2014). Recently, we developed diverse organoselenium agents with potential antioxidant activities. Of interest, pseudo-peptidic organoselenium **III** and **IV** exhibited good GPx-like activity (up-to 2.5 folds higher than ebselen) and antioxidant activity similar to vitamin C (Shaaban et al., 2019; Shaaban et al., 2016) (Fig. 1). Moreover, the Selenium-based *N*-substituted maleanilic acids (**V** and **VI**) showed potential antioxidant activity comparable to vitamin C, GPx-like activity like ebselen, and interesting anti-apoptotic properties in OLs (Shaaban et al., 2016; Shaaban et al., 2019; Cherkaoui-Malki et al., 2019) (Fig. 1).

Interestingly, these agents are carboxylates in nature, which are often unfavorable from a pharmacological perspective as they have low permeability through biological membranes, are poorly absorbed orally, and are rapidly cleared. Therefore, bioisosteric substitution is used in drug development to generate more tolerated surrogates of lead structures (Myznikov et al., 2007). On the other, several nitrogen heterocyclic compounds have shown a wide range of pharmacological activities (e.g., anticancer) and were also used as carboxylic acid surrogates. Tetrazoles are amongst the most frequently used carboxylic acid isostere. Indeed, they are the core scaffolds of many marketed drugs (e.g., cilostazol, cefazoline, ceftazole, alpidem, and olprinone) and have broad application in organometallic and coordination chemistry (Myznikov et al., 2007; Song et al., 2013; Lacerda et al., 2014). Additionally, tetrazoles have similar planarity and acidity to carboxylic acid, but they are larger and more lipophilic (\approx ten times). These, in turn, facilitate their crossing through the blood-brain-barrier (Song et al., 2013; Shmatova and Nenajdenko, 2013; Ostrovskii et al., 2013).

Given the above, a key objective was to develop carboxylic acid isostere organoselenium compounds (likely, nitrogen-heterocyclic such as tetrazoles) to improve their respective pharmacokinetics. Accordingly, we developed tetrazole-derived organic diselenides **VII** and **VIII**, which exhibited enhanced GPx-like activity to ebselen (up-to five folds) and scavenging free-radical property similar to ascorbic acid (Shaaban et al., 2016; Shaaban et al., 2019). Furthermore, the tetrazole-based quinone **IX** showed potential anti-

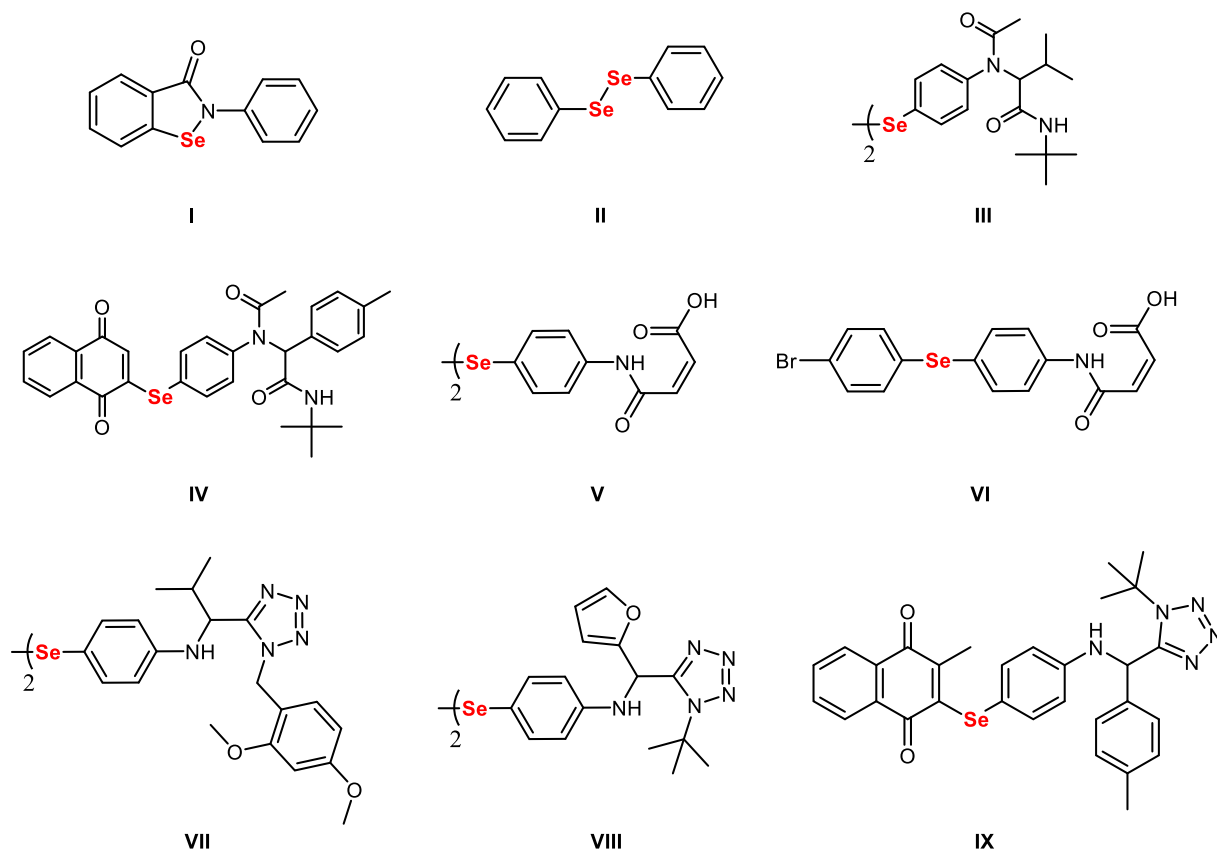


Fig. 1 Structures of functionalized organoselenium compounds with promising anticancer and antioxidant activities.

HepG2 activity via the downregulation of the Ki-67 and Bcl-2 levels and activation of caspase-8 in HepG2 cells (Shaaban et al., 2016; Shaaban et al., 2019). These tetrazole-based organoselenium compounds provided a promising starting point for structure diversification and activity modifications (Shaaban et al., 2016; Shaaban et al., 2015; Shaaban et al., 2016; Shaaban et al., 2019; Cherkaoui-Malki et al., 2019).

Collectively, our previous studies have shown promising antioxidant activities of the organoselenium compounds in human cancer cells. Therefore, we are now interested in moving this line of investigations into studies in OLs to establish a complete image of organoselenium compounds as proper cytoprotective agents. Based on our ongoing efforts in developing bioactive organoselenium compounds, we herein aim to develop novel tetrazole- and pseudopeptide-based organoselenium compounds of expected antioxidant and cytoprotective activities for the myelin-forming cells, OLs.

The synthesis was conducted via the isocyanide-based multicomponent reactions (IMCRs) as part of the Diversity Oriented Synthesis (DOS). (Lacerda et al., 2014; Rivera et al., 2014) Although IMCRs give access to a diverse and considerable number of compounds, our main objective is to perform more extensive biological investigations on a novel and a small number of compounds rather than expand the organoselenium chemical space. Furthermore, cellular *in vitro* investigations were also carried out using murine immortalized 158 N and 158JP OLs. The ROS levels were evaluated using the hydroethidine (DHE) and the 2',7'-dichlorodihydrofluorescein diacetate (H2-DCFDA) assays using flow cytometry. Moreover,

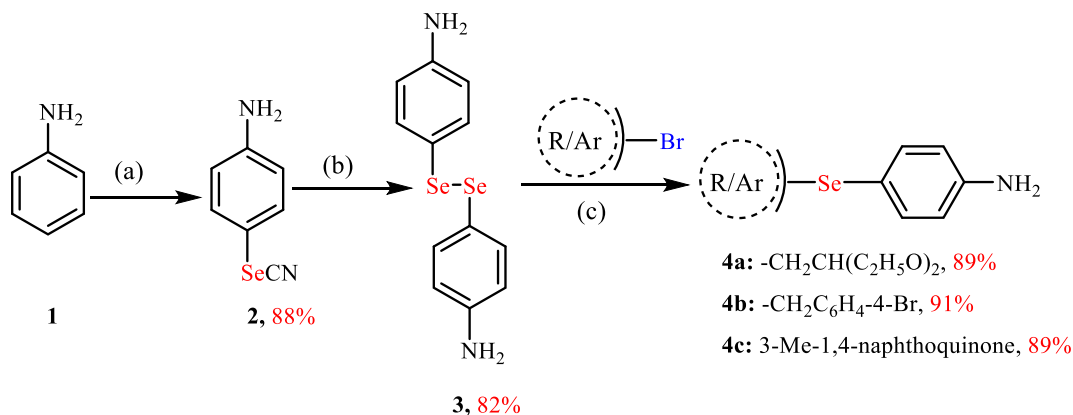
the synthesized organoselenium compounds' redox potentials were investigated employing different *in vitro* assays such as the GPx-like activity, azBTS-(NH₄)₂ (ABTS), bleomycin-induced DNA damage, and 2,2-diphenyl-1-(2,4,6-trinitrophenyl)hydrazyl (DPPH) chemical assays. Additionally, the redox properties of newly synthesized organoselenium compounds were also explored using advanced computational tools for the docking process. This *in-silico* assay aims to simulate inhibition activity as well as strengthen *in-vitro* results.

2. Results and discussion

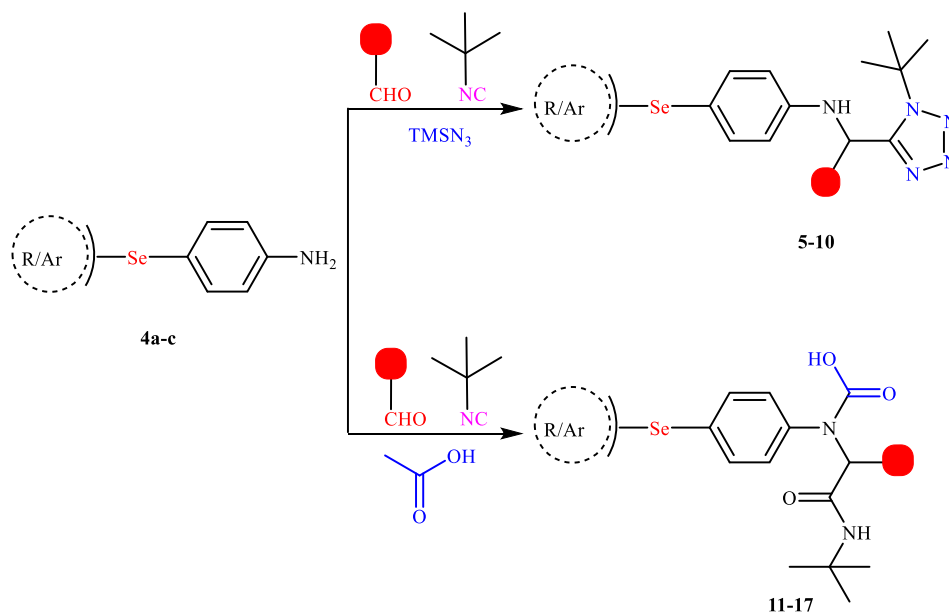
2.1. Design and synthesis

The synthesis of organoselenium compounds has recently witnessed significant interest. Mainly because they showed potential antioxidant and neuroprotective activities against some neural injury models. (Miller, 2019; Lenardão et al., 2018; Krief and Hevesi, 2012) IMCRs have been used to synthesize diverse biologically active organoselenium compounds; however, the scope is limited by the availability of selenium-based building blocks. Amines are the most common and versatile building blocks among several IMCRs (e.g., Groebke-Blackburn-Bienaymé, Ugi, and azido-Ugi reactions). Therefore, three selenium-based anilines **4a-c** were synthesized and their reactivities were explored in the Ugi and azido-Ugi reactions to develop novel tetrazole- and pseudopeptide-based organoselenium compounds of expected antioxidant and cytoprotective activities for the myelin-forming cells, OLs.

4-Selenocyanatoaniline (**2**), 4,4'-diselanediyldianiline (**3**), and selenium-based amines **4a-c** were synthesized according to our reported method (Shaaban et al., 2019). Initially, 4-selenocyanatoaniline (**2**) and 4,4'-diselanediyldianiline (**3**) were synthesized starting from aniline and triselenium dicyanide. The selenium-based amines **4a-c** were thereafter prepared by the reduction of 4,4'-diselanediyldianiline (**3**) with sodium borohydride followed by subsequent nucleophilic substitution (S_N) reactions at different halo-derivatives (e.g., bromoacetaldehyde diethyl acetal, 4-bromobenzyl bromide, or 2-bromo-3-methylnaphthoquinone) (Scheme 1) (Shaaban et al., 2019).



Scheme 1 Synthesis of the organoselenium-based amines **4a-c**. Reagents and conditions: (a) SeO_2 (2.4 mmol), malononitrile (1.2 mmol), aniline (2 mmol), DMSO (2 ml); (b) NaBH_4 (6 mmol), 4-selenocyanatoaniline **2** (2 mmol), EtOH (10 ml); (iii) Halo-derivative (1.1 mmol), aliquat 336 (5% mol), NaBH_4 (3 mmol), EtOAc: H₂O (1:1).



Scheme 2 Synthesis of organoselenium compounds via Ugi and azido-Ugi reactions. Reagents and conditions: Tetrazole-based organoselenium compounds (**5-10**): amine (1 mmol), aldehyde (1.1 mmol), acid (1.1 mmol), and isocyanide (1.1 mmol); CH_2Cl_2 (1 ml), twenty-four hr. Peptidomimetic organoselenium compounds (**11-17**): amine (1 mmol), aldehyde (1.1 mmol), TMSN_3 (1.1 mmol), and isocyanide (1.1 mmol), MeOH (1 ml), twenty-four hr.

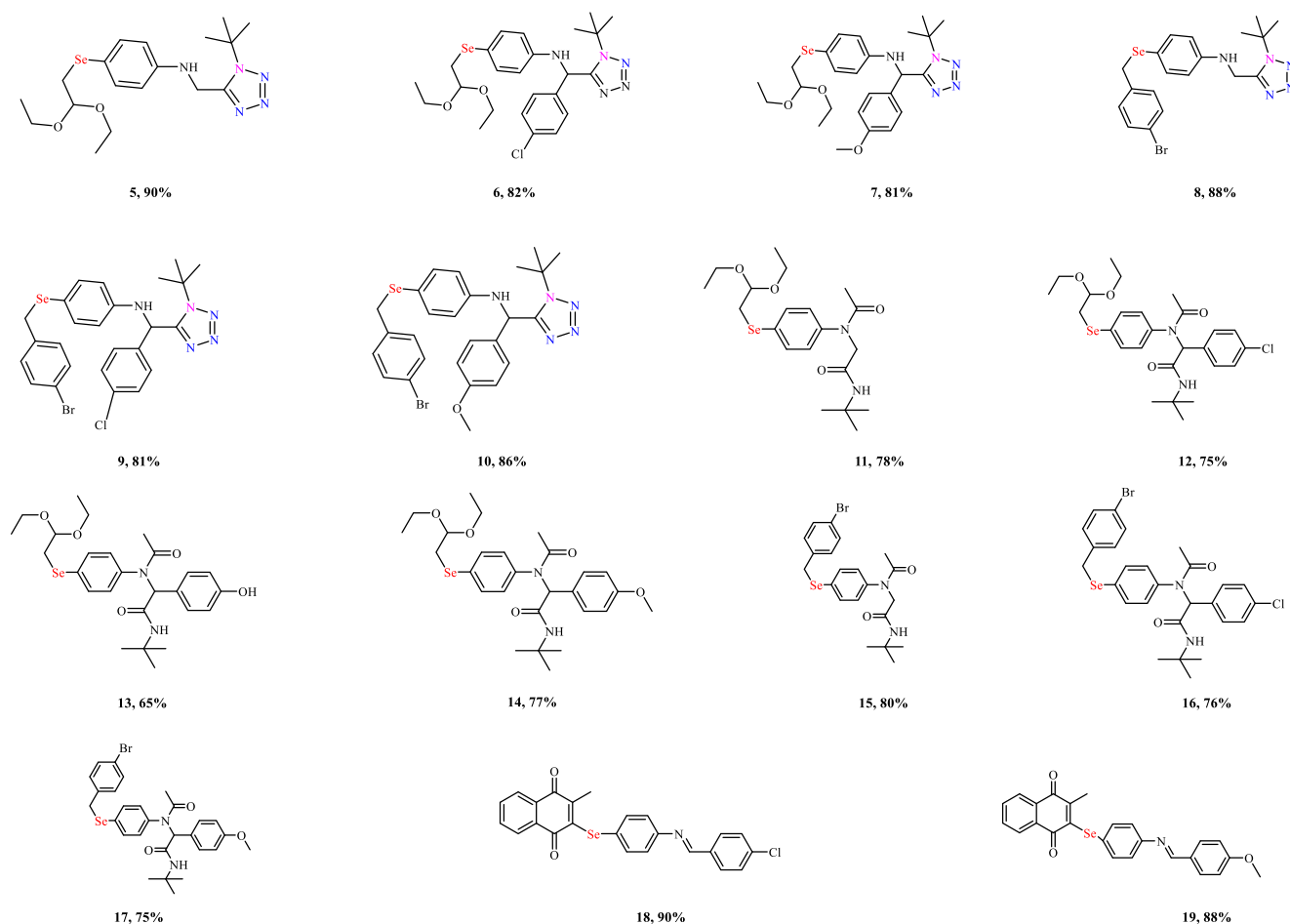


Fig. 2 Chemical structures of the organoselenium compounds (**5–17**) synthesized via U-4CR as well as the selenoquinone-based Schiff bases **18** and **19**.

reaction sequence was initiated by the one-pot addition of the amine to the aldehyde in methanol followed by subsequent addition of *tert*-butyl isocyanide and carboxylic acid/TMSN₃.

The reactions worked well with selenoamines **4a** and **4b** and the corresponding tetrazoles- (**5–10**) and pseudopeptides-based (**11–17**) organoselenium were synthesized in good yields (up to 90% and 80%, respectively) (Fig. 2). Surprisingly, the selenoquinone-based amine **4c** did not afford the desired tetrazoles/pseudopeptides under these conditions, but after a long time of stirring, the selenoquinone-based Schiff bases **18** and **19** were only isolated. Next, the reaction was performed using the isolated selenoquinone-based Schiff bases which also failed. This probably due to their low basicity/nucleophilicity of the Schiff bases. This in turn limited the number of compounds as for the combinatorial approach.

Noteworthy, aromatic aldehydes with the methoxy and chlorine electron-donating groups afforded the tetrazoles/pseudopeptides derivatives in higher yields (up to 86% and 82%, respectively) than 4-hydroxybenzaldehyde (55%). The latter led to the expected products though with lower yield probably due to the competition between the Mumm and Smiles rearrangements.

2.2. Biology

2.2.1. The effect of tetrazole- and pseudopeptide-based organoselenium compounds on the proliferation of the 158 N and 158JP OLs

OLs secure fast signal conduction along the neurons via the myelination and insulation of their axons. (Bechler and Byrne, 2015; Edgar and Sibille, 2012; Feutz et al., 2001) The CNS's most vulnerable cells to ROS are OLs and despite the potential chemopreventive and antioxidant activities of organoselenides, their cytoprotective role on OLs was scarcely explored so far (Cherkaoui-Malki et al., 2019; Baarine et al., 2009; Zarrouk et al., 2012). We are now therefore interested to explore the cytoprotective activity of the newly prepared organoselenium compounds on 158JP and 158 N OLs. Noteworthy, 158JP jimpy cells were selected as a model system for the cytoprotection as it is mutated in the myelin protein PLP/DM20 which maintains myelin sheaths. The basal OLs cytotoxicity was evaluated using MTT assay and 7-ketocholesterol (7kc) as the positive control (Vejud et al., 2005). The IC₅₀s were initially estimated and the corresponding noncytotoxic concentrations were subsequently selected for further cytoprotection investigations (Table 1).

Table 1 Influence of organoselenium compounds on the proliferation of 158 N, and 158JP OLS.^a

Compd. No.	In vitro Cytotoxicity IC ₅₀ (μM)	
	158 N	158JP
7Kc	37 ± 0.5	74 ± 0.9
4a	54 ± 0.8	<i>b</i>
4b	<i>b</i>	<i>b</i>
4c	27 ± 0.3	<i>b</i>
5	78 ± 0.7	<i>b</i>
6	<i>b</i>	<i>b</i>
7	<i>b</i>	<i>b</i>
8	58 ± 0.9	<i>b</i>
9	58 ± 0.8	<i>b</i>
10	32 ± 0.6	<i>b</i>
11	<i>b</i>	<i>b</i>
12	77 ± 0.9	<i>b</i>
13	<i>b</i>	<i>b</i>
14	<i>b</i>	<i>b</i>
15	<i>b</i>	<i>b</i>
16	57 ± 0.8	<i>b</i>
17	<i>b</i>	<i>b</i>
18	26 ± 0.5	<i>b</i>
19	<i>b</i>	<i>b</i>

^aThe MTT assay used to estimate the viability of the cells after 24 h treatment with several concentrations of organoselenium compounds (0, 1, 10, 20, 50, and 100 μM). The IC₅₀ is the mean of two parallel experiments; the positive control is 7Kc.

^bInhibition of cell-growth was not observed.

At the concentration range used, none of the compounds manifested any cytotoxicity (IC₅₀ ≥ 100 μM), except for the selenoquinone amine **4c** and the selenoquinone Schiff base **18**. These two quinone-based compounds were more cytotoxic to 158 N cells (IC₅₀ = 27 μM for compound **4c** and 26 μM for compound **18**) than 7Kc (IC₅₀ = 37 μM). This was not surprising since quinones act as ROS-generators (e.g., superoxide radical anion (O₂⁻) and peroxide) via redox cycling with triplet oxygen. (Zubair et al., 2013; Bair et al., 2010; Kiran Aithal et al., 2009) Furthermore, the selenoamines **4a** (IC₅₀ ≥ 54 μM), the tetrazole-based compounds **5** (IC₅₀ ≥ 78 μM), **8** (IC₅₀ ≥ 58 μM), and **9** (IC₅₀ ≥ 58 μM), and the peptide-based Ugi adducts **12** (IC₅₀ ≥ 77 μM) and **16** (IC₅₀ ≥ 57 μM) exhibited moderate-low cytotoxicities. These compounds are slightly more amphiphilic and hence might be more up-taken by 158 N cells and are expected to exhibit prooxidant activities.

2.2.2. Assessment of the redox properties of the tetrazole- and pseudopeptide-based organoselenium compounds on OLS

The redox status of the organoselenium compounds environment (oxidizing or reducing) decides whether they behave as prooxidants or antioxidants, respectively (Miller, 2019; Lenardão et al., 2018; Shaaban et al., 2014). Generally, they act as antioxidants under redox homeostatic conditions i.e. normal cells. The plausible reason for their apparent antioxidant, in this case, is due to their good nucleophilicity (Krief and Hevesi, 2012; Xu et al., 2020; He et al., 2020; Cardoso et al., 2015; Shaaban et al., 2014; Sharma and Amin, 2013; Sanmartin et al., 2012). On the other hand, they turn to be prooxidants in oxidatively stressed cells (Galant et al., 2020; Chen et al., 2020; Nogueira and Rocha, 2011; Doering et al.,

2010). Considering that the OLS are prone to damage by ROS, our objective is to evaluate the redox properties of the newly synthesized organoselenium compounds using different biochemical (e.g., H2-DCFDA and DHE) and chemical assays (e.g., GPx, ABTS, DPPH, and Bleomycin DNA damage).

2.2.2.1. Estimation of ROS production using H2-DCFDA and DHE assays.

H2-DCFDA and DHE assays are among the most used methods to evaluate the endogenous ROS levels. H2-DCFDA probe is used to detect several types of ROS such as peroxides, peroxy nitrates, and lipid hydroperoxides. DHE is only used for the detection of O₂⁻. (Karlsson et al., 2010; Nury et al., 2014)

Therefore, H2-DCFDA and DHE assays were used to evaluate the ROS levels upon treatment of 158 N cells with the tetrazole- and pseudopeptide-based organoselenium compounds using flow cytometry (Fig. 3).

In the case of the H2-DCF assay, the tetrazole- **6**, **7**, and **9** and the pseudopeptide-based **15** and **17** organoselenium compounds displayed antioxidant properties by lowering the ROS production. Surprisingly, all these compounds did not exhibit any apparent cytotoxicity against 158 N and 158JP OLS, except for the tetrazole-based organic selenide **9**, which only exhibited moderate toxicity in 158 N cells (IC₅₀ ≥ 58 μM). These compounds have interesting cytoprotective and antioxidant activities and are therefore considered as potential myelin diseases drug candidates.

On the other hand, the quinoid-based compounds **4c** and **18** exhibited potential prooxidant activity via increasing the ROS levels in 158 N cells (Fig. 3). This might be explained by the catalytic ability of quinones to reduce dioxygen and generate O₂⁻. The later often converted to other more cytotoxic ROS able to induce oxidative damage, and cell death likely via an apoptosis-mediated pathway. (Zubair et al., 2013; Bair et al., 2010; Kiran Aithal et al., 2009) Furthermore, the tetrazole-based organic selenide **5** and the pseudopeptide-based organoselenium compounds **12** and **14** showed also prooxidant activity by inducing ROS overproduction at all the tested concentrations.

In the case of the DHE assay, the tetrazole- **5**, **6**, and **7** and the pseudopeptide-based **11** and **15** organoselenium compounds showed potential antioxidant properties via decreasing the O₂⁻ levels in 158 N cells. Interestingly, the selenopseudopeptide **11** displayed the most promising antioxidant effect (90% decrease) compared to vitamin E. Furthermore, the selenotetrazole **5** exhibited similar antioxidant activity to the selenopseudopeptide **11** however at 50 μM.

On the other hand, the quinoid-based compound **4c** and the pseudopeptide-based organoselenium compounds **12**, **14**, and **17** exhibited prooxidant activities by increasing the O₂⁻ levels in a concentration-dependent manner (Fig. 4).

2.2.2.2. Estimation of the antioxidant properties.

The *in vitro* ABTS and DPPH methods are routinely used to explore the antioxidant properties of food, natural products, bioactive compounds, and drugs. They are simple, sensitive, and rapid spectrophotometric tools and can be therefore performed in organic and aqueous solvent systems at different pH values. (Luchese et al., 2012; Tian and Schaich, 2013)

The antioxidant capacity is estimated by the decolorization of the bluish-green or purple color of the stable ABTS[•] and DPPH[•] radicals, respectively. The corresponding scavenging

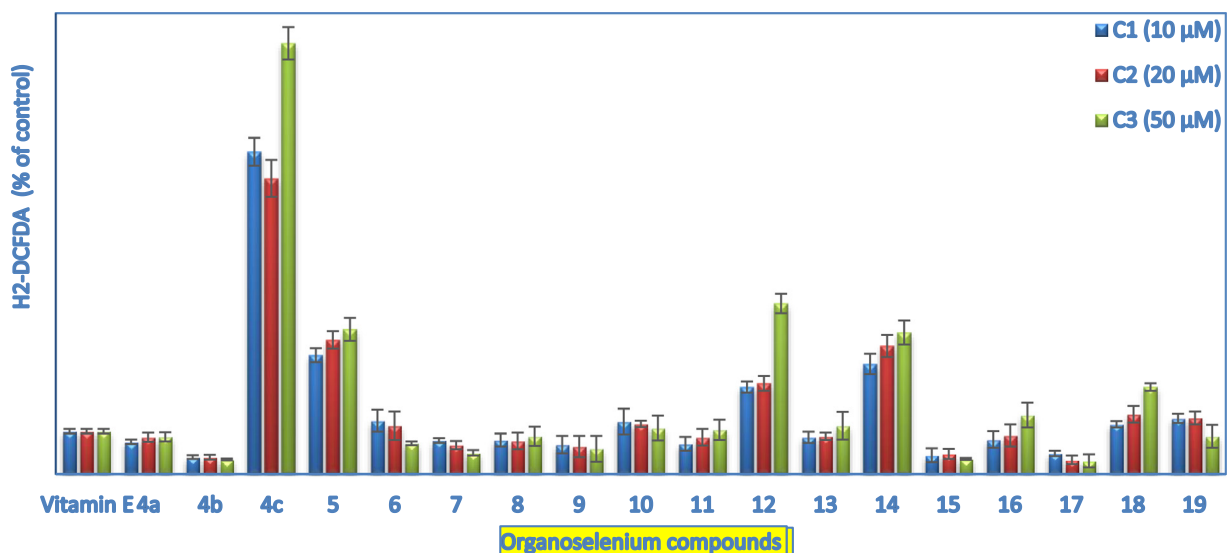


Fig. 3 Estimation of ROS production using H2-DCFDA assay. Positive control is vitamin E (50 μM); ROS levels were followed using flow cytometry. Values are expressed as % control and shown as mean ± S.D, Mann–Whitney test; *: P < 0.05.

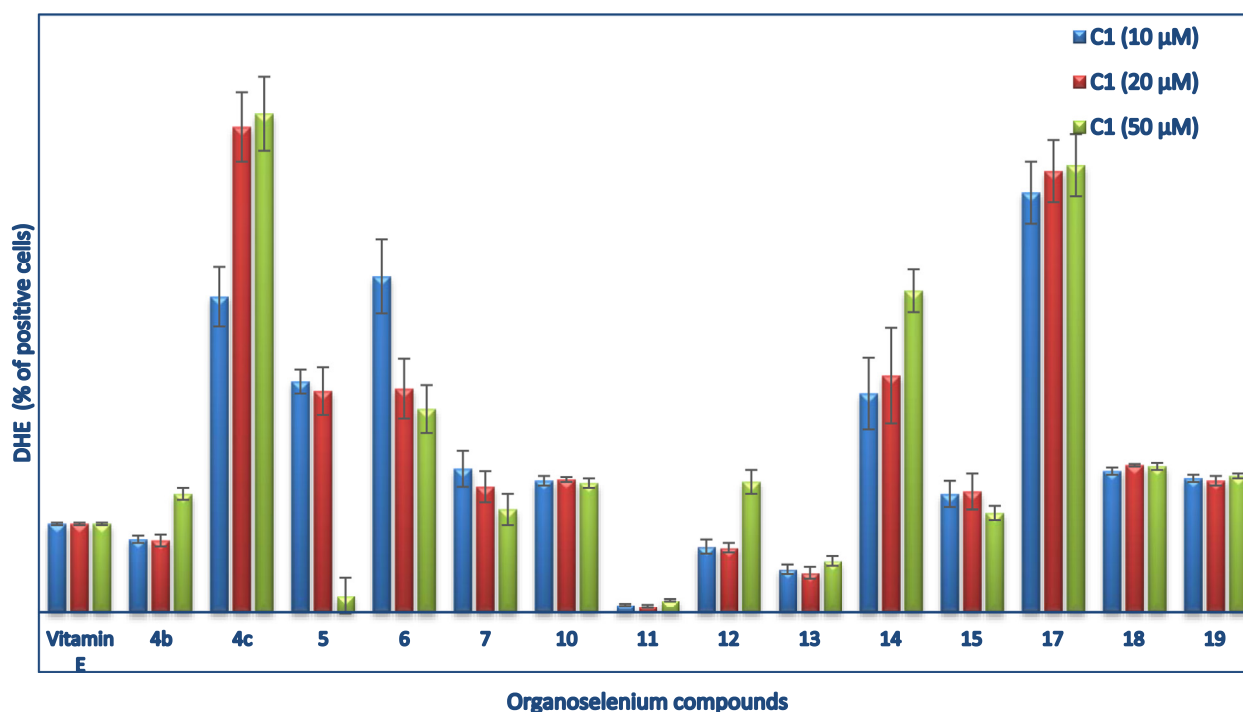


Fig. 4 Estimation of O₂⁻ production using DHE assay. Positive control is vitamin E (50 μM); O₂⁻ levels were followed using flow cytometry technique via staining cells with DHE. Values are expressed as % control and shown as mean ± S.D.; Mann–Whitney test; *: P < 0.05 for treated cells. compounds 4a, 8, 9, and 16 were not tested.

activity (% inhibition) is detected by the extent of absorbance suppression at 734 and 517 nm, using ascorbic acid as the positive control.

As presented in Fig. 5, the quinoid-based organoselenium compounds 4c, 18, and 19 exhibited between 41 and 62% antioxidant activities compared to vitamin C. This was surprising since the selenoquinone 4c and 18 showed potential proox-

idant activities in the H2-DCFDA and DHE assays. Quinones were reported to exhibit antioxidant properties however at lower concentrations. (Mecklenburg et al., 2009; Plano et al., 2011; Shaaban et al., 2012) Furthermore, the ABTS and DPPH methods are only limited for *in vitro* models and shouldn't be admitted before further confirmation by *in vivo* experiments.

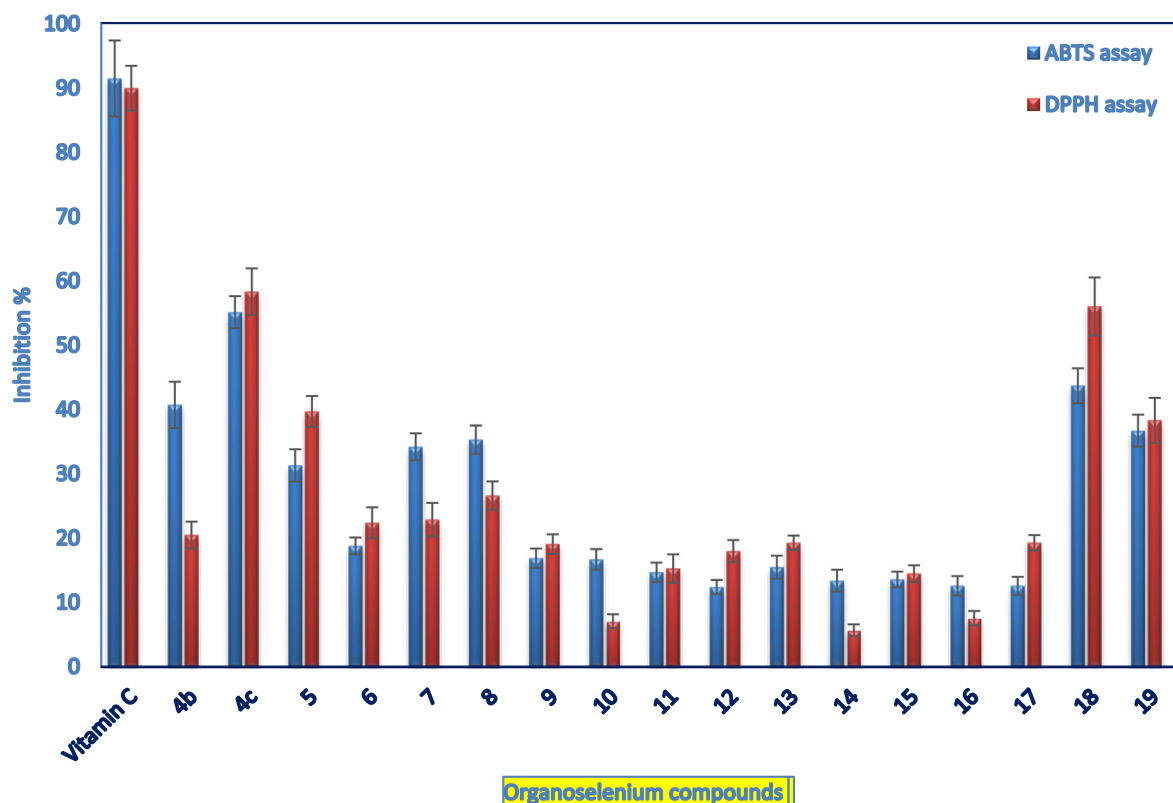


Fig. 5 Estimation of the organoselenium compounds redox properties using the ABTS and DPPH assays. Values are mean \pm SD. DPPH assay: absorbance was read at 517 nm after 30 min of mixing 200 μ L of each compound (1 mM, MeOH) with 400 μ L of DPPH (0.1 mM, MeOH). ABTS assay: 50 μ L of each compound (1 mM, phosphate-buffered methanol) was mixed with ABTS solution (60 mM), and absorbance was monitored at 734 nm. Ascorbic acid was a positive control.

2.2.2.3. *Estimation of the prooxidant properties of the organoselenium compounds using the bleomycin-induced DNA damage assay.* The prooxidant activity of many antineoplastic drugs is commonly evaluated by the DNA strands break using bleomycin-Fe complex method. (Wang et al., 2013; Evans and Halliwell, 1994) The bleomycin antibiotic exhibits antitumor activity via DNA cleavage upon complexation with ferrous cations. The prooxidant activity is estimated by the reduction of bleomycin-Fe(III) to bleomycin-Fe(II) and subsequent degradation of DNA. The extent of the latter is estimated by absorbance increase at 532 nm (Table 2) (Mira et al., 2013).

Prooxidant activity was only noticed by the pseudopeptide-based organic selenide **12** which in turn promoted DNA degradation by the reduction of bleomycin-Fe(III) to bleomycin-Fe(II). This was in good agreement with the H₂-DCFDA and DHE assays.

2.2.2.4. *GPx-like activity assay.* The GPx selenoenzyme catalyzes the reduction of peroxides and lipid hydroperoxides to water and alcohol, respectively. The reaction occurs at the catalytic site of the enzyme i.e. the selenium center at the selenocysteine residue. The latter is an essential cofactor for the antioxidant activities of all the mammalian GPx types (Haselton et al., 2015; Shaaban et al., 2016; Stralioetto et al., 2013). Organoselenium compounds are well-known mimics of the GPx selenoenzyme. They are chemically and metaboli-

cally stable than the GPx itself and this increased the concern in the rational design of novel organoselenium agents as GPx mimics. Recently, we reported different organoselenium agents with GPx-like activity more than ebselen. (Shaaban et al., 2016; Shaaban et al., 2015; Shaaban et al., 2016; Shaaban et al., 2019; Cherkaoui-Malki et al., 2019) Therefore, we evaluated the GPx mimicking activity of novel organoselenium compounds using ebselen as a positive control.

The NADPH-reductase coupled assay was employed to estimate the catalytic GPx mimic activity of the novel organoselenium compounds. (Shaaban et al., 2019; Cherkaoui-Malki et al., 2019) Ebselen was used as a positive control. The GPx-like activity was monitored after the correction of the background reaction of H₂O₂ with GSH. The reaction rate was consistently linear, and the reaction was followed until completion (Fig. 6).

As shown in Fig. 6, most of the organic selenides showed moderate-good GPx-like properties, in particular, the tetrazole- **5** and **9** and the selenopeptide **11** and **15** organoselenium compounds. This was in accordance with the results obtained from the H₂-DCFDA and DHE assays. Interestingly, the selenoquinone **4c** exhibited an interesting GPx activity. Again, this was not expected since the selenoquinone **4c** showed potential prooxidant activity in the H₂-DCFDA and DHE assays. Recently, we have reported quinones with antioxidant activities however at low concentrations. (Mecklenburg et al., 2009; Plano et al., 2011; Shaaban et al., 2012) Further-

Table 2 Estimation of the prooxidant properties of organoselenium compounds.

Compound No.	Bleomycin-dependent DNA damage assay	
	Absorbance	Fold
4b	321 ± 2.7	0.5
4c	483 ± 4.3	0.8
5	396 ± 2.2	0.6
6	361 ± 3.6	0.6
7	537 ± 5.7	0.9
8	187 ± 1.5	0.3
9	508 ± 5.4	0.8
10	505 ± 5.3	0.8
11	592 ± 4.8	0.9
12	714 ± 6.4	1.1
13	337 ± 2.5	0.5
14	390 ± 2.9	0.6
15	470 ± 3.6	0.8
16	321 ± 2.7	0.5
18	212 ± 2.8	0.3
19	490 ± 2.1	0.8
Vitamin C	620 ± 2.6	1

Measurements are mean ± SD.

more, the pseudopeptide- **12** and the selenoquinone **18** organoselenium compounds exhibited lower GPx activities compared to the other examples in the series.

2.3. Simulation for the behavior of chosen compounds towards significant proteins

In-silico molecular studies are often applied as confirmatory tools of the antioxidant/prooxidant properties of drug candidates. The redox properties of the most interesting organoselenium compounds were further explored via advanced computational tools for the docking process using Molecular

Operating Environment-docking (MOE) studies. The latter is utilized to assert the biological results from a theoretical point of view and evaluate the extent of conformity. The tetrazole-based organic selenide **9** and the pseudopeptide-based organoselenium compounds **11** and **15** were selected for this simulation because of their good antioxidant and GPx activities. On the other hand, the quinone-based **4c** and the pseudopeptide-based **12** organoselenium compound were chosen due to their prooxidant activity as well as their low GPx properties which in turn is important for comparison studies (see 2.3 part). Therefore, chosen organoselenium compounds likewise reference antioxidant ebselen, were analyzed by MOE docking versus two kinds of proteins (2F8A and 3C1L). Consequently, 2F8A is a GPx protein, which routinely screened to assess the extent of similarity to glutathione peroxidase (Mashat et al., 2019). Whereas, 3C1L is a free radical booster protein, which is tested to develop a comparative view of antioxidant behavior for new compounds (Al-Hazmi et al., 2020; Al-Hazmi et al., 2019; Al-Hazmi et al., 2020). Therefore, the docking patterns (Figs. 7 and 8, S1, and S2) as well as interaction parameters (Table 3), which exported after docking execution, were displayed and discussed in terms of the following: i) The influential contributing sites N11, 16; O11, 19, and 6-ring, ii) The bonded amino acid residues LYS30, 80; ARG89; PRO28, 105, and GLU116, which considered the receptors for docking sites, iii) The allosteric binding H-acceptor, H-donor, and pi-H, which contributes to docking paths, and iv) Concerning docking within 3C1L protein, effective docking paths (≤ 3.5 Å) were recorded excellently with **9**, **11**, and ebselen compounds, which denote their superior antioxidant activity. Moreover, scoring energy values (Kcal/mol) for docking-poses versus 3C1L, support the superiority of compounds **9**, **11**, and ebselen.

Interestingly, the tetrazole-based organic selenide **9** and the pseudopeptide-based organic selenide **11** and ebselen refrained to interact with the 2F8A protein completely. This behavior reflects the potential GPx-like activity of such compounds.

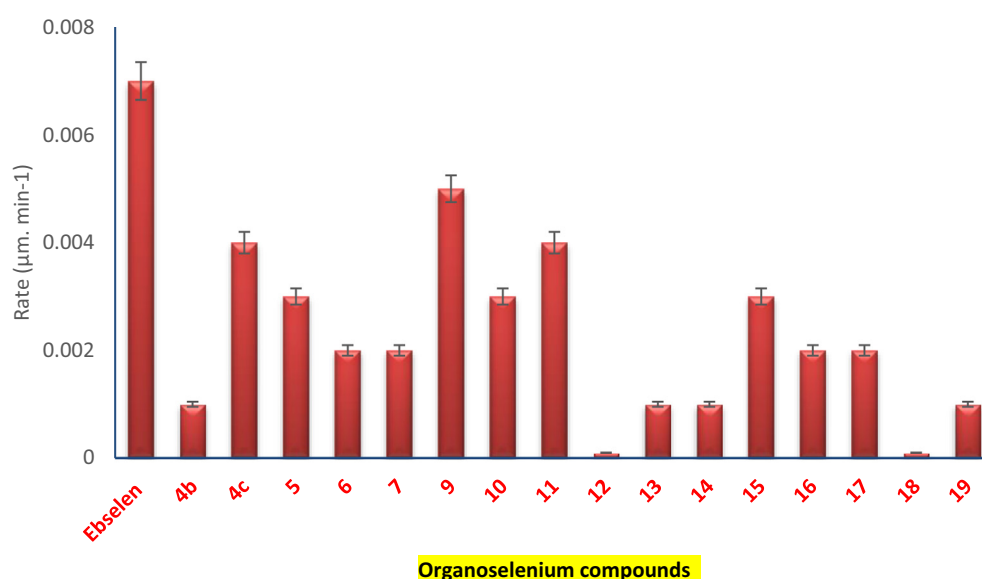


Fig. 6 GPx-like activity assay. During the reaction time-course, a linear reaction rate was observed. The absorbance was recorded at wavelength 340 nm and then $A_{340\text{nm}}/\text{min}$ was calculated. The known, standard GPx mimic compound.

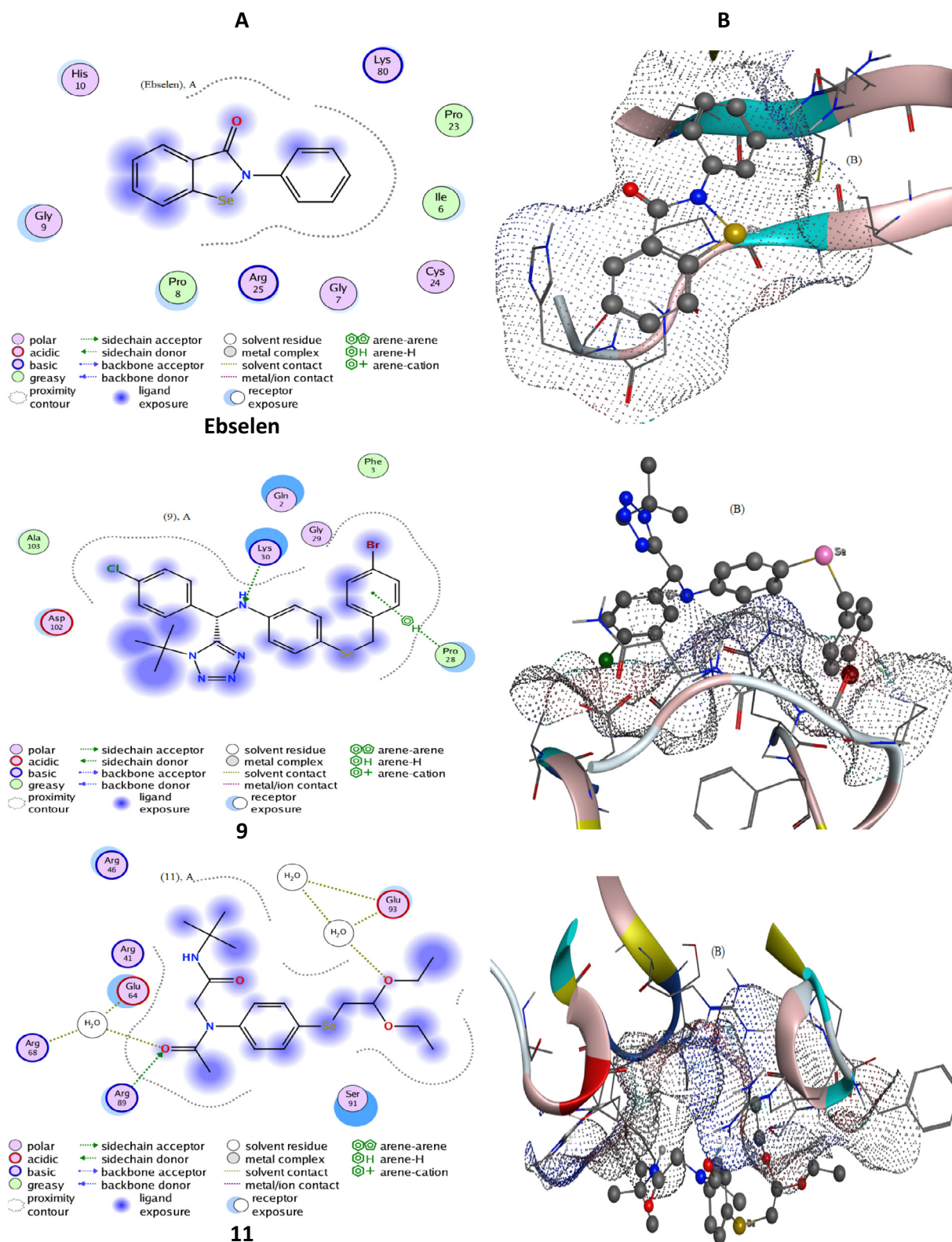


Fig. 7 Docking patterns (panel A) and surface maps (panel B) for selected conformers of compounds **9** and **11** and ebselen against 3C1L protein.

In addition to, extracted docking validity patterns (Figs. 7 and 8, S1, and S2) offer a further confirmation for the previous explanation as follow; i) Regarding 3C1L docking-poses, a

suitable proximity contour appeared with **9**, **11**, and ebselen. Such contour surrounds the evaluable sites which can add extra-binding with receptors. ii) Extended compound exposed

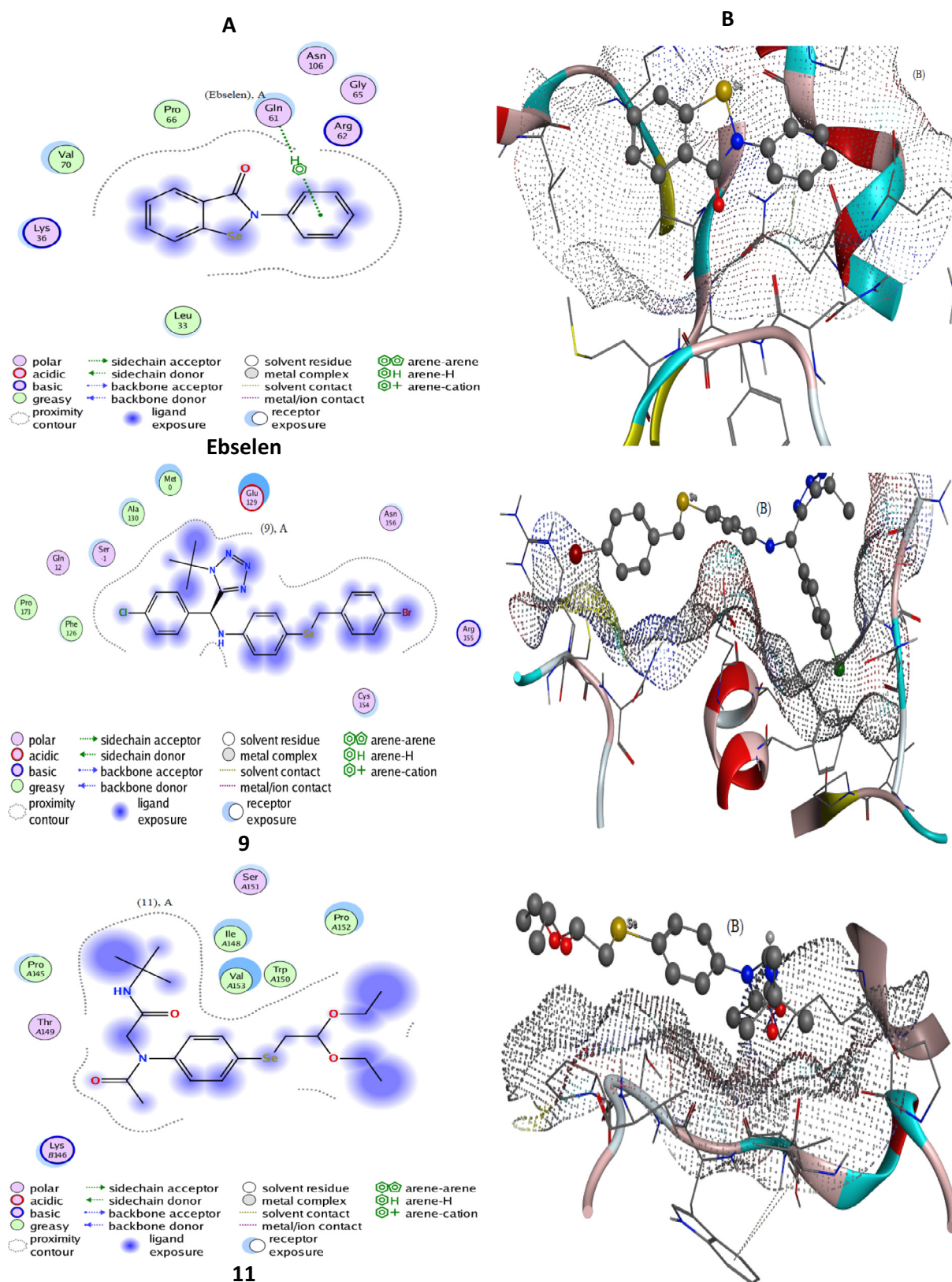


Fig. 8 Docking patterns (panel A) and surface maps (panel B) for selected conformers of compounds **9** and **11** and Ebselen against 2F8A protein.

Table 3 Speculative interaction for selected compounds either antioxidant or against glutathione peroxidase.

Organic selenides	Proteins	Ligand	Receptor	Interaction	Distance (Å)	E (Kcal/mol)	S (energy score)
4c	3C1L	6-ring 6-ring	O HOH 530 (A) O HOH 530 (A)	pi-H pi-H	3.74 3.79	-0.6-0.6	-4.759
	2F8A	—	—	—	—	—	-5.0883
9	3C1L	N11 6-ring	NZ LYS 30 (A) CB PRO 28 (A)	H-acceptor pi-H	3.17 4.28	-9.0-0.9	-5.2081
	2F8A	—	—	—	—	—	-4.8359
11	3C1L	O11 O19 O19	O HOH 510 (A) NH1 ARG 89 (A) O HOH 569 (A)	H-acceptor H-acceptor H-acceptor	3.47 2.96 3.53	-0.6-3.5-0.8	-5.1033
	2F8A	—	—	—	—	—	-5.1641
12	3C1L	N25 C9	OE2 GLU 116 (A) 5-ring TRP 121(A)	H-donor H-pi	3.68 4.21	-1.0-1.0	-5.7548
	2F8A	—	—	—	—	—	-5.7796
15	3C1L	6-ring	NZ LYS 80 (A)	pi-cation	3.75	-1.1	-5.5094
	2F8A	N16	O PRO 105(A)	H-donor	3.09	-1.1	-5.9015
Ebselen	3C1L	6-ring	CG GLN 61(A)	pi-H	3.50	-0.6	-4.92541
	2F8A	—	—	—	—	—	-4.1646

surface appeared with the quinone-based **4c** and the pseudopeptide-based **12** organoselenium compounds on behalf of that of the receptor exposed surface. iii) Backbone donors and acceptors were the main receptors contributing to true paths. On the other hand, and regarding 2F8A dockings, a good proximity contour surrounds the compound and prevents facilitating interaction with receptors. An extended compound exposed surface was recorded with all docking organoselenium compounds, which signify the absence of interaction at all. (Al-Hazmi et al., 2020; Al-Hazmi et al., 2019; Al-Hazmi et al., 2020) iii) In addition to complete shrinkage for receptor exposed surface in all organoselenium compounds, which attached reversely. Collectively, the *in silico* studies were in good agreement with the experimental results and show that the tetrazole-based organic selenide **9** and the pseudopeptide-based organoselenium compounds **11** and **15** have good antioxidant and GPx activities. On the other hand, the quinone-based **4c** and the pseudopeptide-based **12** organoselenium compounds have low antioxidant activity.

2.4. Quantitative structure–property relationships (QSAR)

Next, the drugability of the quinone-based **4c**, tetrazole-based organic selenide **9**, and the pseudopeptide-based organoselenium compounds **11**, **12**, and **15** were *in silico* explored using HyperChem (8.1) software. The latter is used to estimate different pharmacokinetic and physicochemical parameters. These in turn reflect the relationship between molecular structure and attributes. Selected conformers of compounds **4c**, **9**,

11, **12**, and **15** as well as ebselen as a reference, were faced optimization process. Configuration was started by adding hydrogen atoms, setup Molecular mechanics (MM⁺), and semi-empirical (AM1), then energy minimization proceeded. The method was executed with free parameters under the “Polake-Ribiere conjugated gradient-algorithm” (Althagafi et al., 2019). Hydration energy, reactivity, partition coefficient (log P), volume, and surface area were then computed (Table 4). Regarding surface area and volume that directly reflect the catalytic behavior, it appeared high with most of the compounds. This in turn points to their influential catalytic feature, which preferable in various applications (e.g., redox properties). Interestingly, organoselenium compounds **11** and **15** exhibited higher hydration energy and log P over ebselen. This in turn proposes superior pharmacokinetics of compounds **11** and **15** than ebselen (Al-Hazmi et al., 2019; Al-Hazmi et al., 2020).

3. Conclusions

The synthesis of novel peptide-like and tetrazole-based organoselenium compounds was carried out via Ugi and Ugi-azide IMCRs, respectively. The cytoprotective properties of the newly prepared seleno organic compounds were investigated against 158 N and 158JP OLs. Most of the organoselenium compounds did not show any cytotoxic influence on 158JP. The same holds in the case of 158 N cells, except for selenoquinone **4c** (IC₅₀ ≥ 27 μM), and **18** (IC₅₀ ≥ 26 μM).

In the H2-DCF and DHE assays, the tetrazole-based organoselenium compounds **6**, **7**, and **9** and the

Table 4 QSAR data for selected compounds.

The parameters	4c	9	11	12	15	Ebselen
Surface area (grid) (Å)	432.06	631.73	598.16	721.15	570.00	345.16
Volume(Å)	827.02	1309.23	1206.98	1423.48	1154.28	673.60
Hydration energy (k cal/mol)	-7.97	-9.95	-0.73	-1.47	-1.91	-3.44
Log p	-0.25	2.80	-0.86	0.12	-0.49	0.00
Reactivity(Å)	86.97	150.30	106.80	140.01	116.76	66.79

pseudopeptide-based organoselenium compounds **11**, **15**, and **17** showed potential antioxidant properties via decreasing ROS levels. On the other hand, the quinoid-based compound **4c** and the pseudopeptide-based organoselenium compounds **12**, **14**, and **17** showed prooxidant activity by increasing ROS intracellular levels.

Notably, most of the organoselenium agents exhibited low-moderate antioxidant activity compared to vitamin C in the ABTS and DPPH assays. In the case of the bleomycin-induced DNA damage assay, a prooxidant activity was only noticed by the pseudopeptide-based organic selenide **12**. Moreover, most of the compounds showed a moderate-good GPx-like activity. In particular, the tetrazole-based organoselenium compounds **5** and **9** and the selenopeptide **11** and **15** showed the most potent GPx activity in this assay. This was in agreement with the results obtained from the H₂-DCFDA and DHE assays.

The computational approach was executed by two different programs (HyperChem and MOE) to indicate the expected pharmacokinetics and biological activity of selected organoselenium compounds (e.g., **4c**, **9**, **11**, **12**, and **15**). QSAR parameters calculated displayed higher hydration energy and log P for compounds **11** and **15**, which reflect their promising lipophilic feature, which preferable in biological efficiency. Besides, MOE docking simulation displayed significant scoring energy values for docking poses with organoselenium compounds **9**, **11**, **12**, and **15**, which exceed the ebselen itself. This result agrees comfortably with experimental outputs, then the biological application was strong and credible enough after such *in silico* assay.

To conclude, most of the organoselenium compounds exhibited a cytoprotective effect and interesting antioxidant on 158JP Ols and therefore might be considered as potential myelin diseases drug candidates.

4. Experimental protocols

4.1. Material and methods

Chemical reagents, TLC plates, and silica gel 60 were purchased from chemical stores. The spectroscopic analysis was recorded at the “Pôle Chimie Moléculaire” de l’Université de Bourgogne (PACSMUB)”. Melting point measured are uncorrected. 2-Methyl-3-bromo-4-naphthoquinone, compound **3**, and organoselenium-based-amines (**4a-c**) were synthesized according to our reported procedures (Shaaban et al., 2019; Mecklenburg et al., 2009; Plano et al., 2011).

4.2. Biology

4.2.1. Cytoprotective assay

MTT assay was performed according to the literature protocol (He et al., 2006; Shaaban et al., 2015; Shaaban et al., 2015).

4.2.2. Estimation of ROS production

The DCF and DHE were conducted according to the literature protocol (Shaaban et al., 2019; Cherkaoui-Malki et al., 2019).

4.2.3. Antioxidant assays

The ABTS, GPx-like activity, bleomycin-dependent DNA damage, and DPPH assays were conducted according to the

literature protocol (Shaaban et al., 2019; Cherkaoui-Malki et al., 2019).

4.3. The technique of docking simulation process towards significant proteins

Applying the Molecular Operating Environmental approach (MOE, Vs. 2015), the interaction between drugs with functional pathogen-protein was simulated. This implementation aims to confirm in-vitro results, so the chosen compounds either that play good antioxidant (**4d**, **9**, **11**, **15**) or that without efficiency (**12**). Besides, and from a comparative point of view, ebselen drug was handled in this simulation, for clarification. By the way, 3C1L and 2F8A were the functional proteins chosen for this case. Where, 3C1L is the PDB crystal structure of putative antioxidant defense protein, while 2F8A is the PDB crystal structure of the selenocysteine to glycine mutant of human GPx (Al-Hazmi et al., 2019; Al-Hazmi et al., 2020). Consequently, to start the docking process, each side (compound & protein) faced orientation steps to be ready for proceeding. First of all, each compound was configured as follows; i) adding hydrogen atoms, starting energy minimization, and then render atomic charges and potential energies. Moreover, other significant parameters were regulated by the MMFF94x force field. So, the oriented compound may be saved as a new database by MDB format. After that and regarding each selected protein, faced sequential orientation steps starting by adding H-atoms over receptor sites. Then, the receptors were connected before fixing the potential energy. The final stage concerning site-finder to fix the active receptors and dummies over the protein helix. Accordingly, the docking process can be started to complete 30 poses for each method. Some of these poses can be rejected immediately that which clashes with the protein. Such poses were adjusted by London dG-scoring function that was already improved twice times by triangle Matcher. True docking path was confirmed in different ways, the most effective one that exported bond lengths of ≤ 3.5 Å (Al-Hazmi et al., 2019). The interaction parameters as well as the docking patterns were extracted for investigation and ranking inhibition activity for tested compounds relative to the reference drug.

4.4. Synthesis

4.4.1. Procedure I: Synthesis of organoselenium peptidomimetic derivatives (5–10) via Ugi reaction

A mixture of amine (1 mmol), aldehyde (1.1 mmol), acid (1.1 mmol), and isonitrile (1.1 mmol) in 1 ml dichloromethane was stirred for 24 hr at 27 °C. Water was added and the dichloromethane layer was separated, dried, and removed. The residue was purified using ligroin: acetic ester (4:3) flash chromatography.

4.4.2. Procedure II: The synthesis of organoselenium based-tetrazoles derivatives (17–II) via Azido-Ugi reaction

A mixture of amine (1 mmol), aldehyde (1.1 mmol), TMSN₃ (1.1 mmol), and isonitrile (1.1 mmol) in 1 ml methanol was stirred for 24 hr at 27 °C. Water was added and the dichloromethane layer was separated, dried, and removed. The residue was purified using ligroin: acetic ester (4:3) flash chromatography.

4.4.3. *N*-((1-(*tert*-butyl)-1*H*-tetrazol-5-yl)methyl)-4-((2,2-diethoxyethyl)selanyl)aniline (**5**)

Compound **5** was prepared following procedure II from 4-((2-ethoxy-3-methoxypropyl)selanyl)aniline **4a** (289 mg, 1 mmol), paraformaldehyde (33 mg, 1.1 mmol), azidotrimethylsilane (146 μ L, 1.1 mmol) and *tert*-butyl isocyanide (125 μ L, 1.1 mmol). Completion was monitored via TLC ligroin: acetic ester = 4:3, R_f = 0.31, purified using silica gel with ligroin: acetic ester = 1:1. White solid; Yield: 384 mg (90%); mp 81–82 °C. ^1H NMR (300 MHz, CDCl_3) δ 7.43 – 7.35 (m, 2H, Ar-H), 6.60 – 6.53 (m, 2H, Ar-H), 4.60 (t, J = 4.4 Hz, 1H, CH), 4.57 (s, 2H, NHCH_2), 3.58 – 3.44 (m, 4H, 2OCH_2), 2.95 (d, J = 5.6 Hz, 2H, SeCH_2), 1.70 (s, 9H, C(CH_3)₃), 1.11 (t, J = 7.1 Hz, 6H, 2CH_3); ^{13}C NMR (75 MHz, CDCl_3) δ 150.73, 145.33, 134.88, 117.00, 113.05, 101.28, 60.73, 60.42, 39.13, 31.19, 28.61, 14.23; MS (ESI): m/z = found 450.21 [M^+ + Na]; calcd. 427.15 [M^+]; HRMS calcd. for $\text{C}_{18}\text{H}_{29}\text{N}_5\text{O}_2\text{Se}$ [M^+ + Na]: 450.139769, found 450.13662 [M^+ + Na]. Anal. Calcd for $\text{C}_{18}\text{H}_{29}\text{N}_5\text{O}_2\text{Se}$ (427.15): C, 50.70; H, 6.86; N, 16.42. Found: C, 50.68; H, 6.84; N, 16.40.

4.4.4. *N*-((1-(*tert*-butyl)-1*H*-tetrazol-5-yl)(4-chlorophenyl)methyl)-4-((2,2-diethoxyethyl)selanyl)aniline (**6**)

Compound **6** was prepared following procedure II from 4-((2-ethoxy-3-methoxypropyl)selanyl)aniline **4a** (289 mg, 1 mmol), 4-chlorobenzaldehyde (155 mg, 1.1 mmol), azidotrimethylsilane (146 μ L, 1.1 mmol) and *tert*-butyl isocyanide (125 μ L, 1.1 mmol). Completion was monitored via TLC ligroin: acetic ester = 4:2, R_f = 0.29, purified using silica gel with ligroin: acetic ester = 3:2. White solid; Yield: 440 mg (82%); mp 92–93 °C. ^1H NMR (300 MHz, CDCl_3) δ 7.33 – 7.26 (m, 3H, Ar-H), 7.23 – 7.17 (m, 2H, Ar-H), 6.52 – 6.40 (m, 2H, Ar-H), 6.01 (d, J = 9.2 Hz, 1H, Ar-H), 4.83 (d, J = 9.2 Hz, 1H, CH), 4.58 (t, J = 5.4 Hz, 1H, CH), 3.59 – 3.35 (m, 4H, 2OCH_2), 2.92 (d, J = 5.6 Hz, 2H, SeCH_2), 1.64 (s, 9H, C(CH_3)₃), 1.08 (t, J = 7.0, 6H, 2CH_3); ^{13}C NMR (75 MHz, CDCl_3) δ 154.68, 145.03, 136.42, 135.73, 134.71, 129.34, 129.05, 118.46, 114.75, 102.29, 61.89, 61.72, 53.62, 32.04, 30.15, 15.21; MS (ESI): m/z = found 560.19 [M^+ + Na]; calcd. 537.14 [M^+]; HRMS calcd. for $\text{C}_{24}\text{H}_{32}\text{ClN}_5\text{O}_2\text{Se}$ [M^+ + Na]: 560.129769, found 560.12776 [M^+ + Na]. Anal. Calcd for $\text{C}_{24}\text{H}_{32}\text{ClN}_5\text{O}_2\text{Se}$ (537.14): C, 53.68; H, 6.01; N, 13.04. Found: C, 53.70; H, 6.03; N, 13.06.

4.4.5. *N*-((1-(*tert*-butyl)-1*H*-tetrazol-5-yl)(4-methoxyphenyl)methyl)-4-((2,2-diethoxyethyl)selanyl)aniline (**7**)

Compound **7** was prepared following procedure II from 4-((2-ethoxy-3-methoxypropyl)selanyl)aniline **4a** (289 mg, 1 mmol), 4-methoxybenzaldehyde (122 μ L, 1.1 mmol), azidotrimethylsilane (146 μ L, 1.1 mmol) and *tert*-butyl isocyanide (125 μ L, 1.1 mmol). Completion was monitored via TLC ligroin: acetic ester = 4:2, R_f = 0.32, purified using silica gel with ligroin: acetic ester = 3:2. White solid; Yield: 431 mg (81%); mp 78–79 °C. ^1H NMR (300 MHz, CDCl_3) δ 7.30 (d, J = 8.5 Hz, 2H, Ar-H), 7.21 – 7.13 (m, 2H, Ar-H), 6.87 – 6.73 (m, 2H, Ar-H), 6.47 (d, J = 8.6 Hz, 2H, Ar-H), 5.98 (s, 1H, NH), 4.76 (d, J = 9.2 Hz, 1H, CH), 4.57 (t, J = 5.7 Hz, 1H, CH), 3.71 (s, 3H, OCH_3), 3.59 – 3.36 (m, 4H, 2OCH_2), 2.92 (d, J = 5.6 Hz, 2H, SeCH_2), 1.61 (s, 9H, C(CH_3)₃), 1.09 (t, J = 7.0, Hz, 6H, 2CH_3); ^{13}C NMR

(75 MHz, CDCl_3) δ 158.80, 144.46, 134.72, 128.80, 128.03, 116.98, 113.77, 113.52, 101.28, 60.71, 57.43, 54.29, 52.90, 31.06, 29.07, 17.43, 14.20; MS (ESI): m/z = found 556.24 [M^+ + Na]; calcd. 533.19 [M^+]; HRMS calcd. for $\text{C}_{25}\text{H}_{35}\text{N}_5\text{O}_3\text{Se}$ [M^+ + Na]: 556.179769, found 556.17857 [M^+ + Na]. Anal. Calcd for $\text{C}_{25}\text{H}_{35}\text{N}_5\text{O}_3\text{Se}$ (533.19): C, 56.38; H, 6.62; N, 13.15. Found: C, 56.36; H, 6.64; N, 13.17.

4.4.6. 4-((4-bromobenzyl)selanyl)-*N*-((1-(*tert*-butyl)-1*H*-tetrazol-5-yl)methyl)aniline (**8**)

Compound **8** was prepared following procedure II from 4-((4-bromobenzyl)selanyl)aniline **4c** (341 mg, 1 mmol), paraformaldehyde (33 mg, 1.1 mmol), azidotrimethylsilane (146 μ L, 1.1 mmol) and *tert*-butyl isocyanide (125 μ L, 1.1 mmol). Completion was monitored via TLC ligroin: acetic ester = 4:3, R_f = 0.31, purified using silica gel with ligroin: acetic ester = 1:1. White solid; Yield: 421 mg (88%); mp 186–187 °C. ^1H NMR (300 MHz, CDCl_3) δ 7.27 – 7.23 (m, 4H, Ar-H), 6.91 – 6.84 (m, 2H, Ar-H), 6.56 – 6.48 (m, 2H, Ar-H), 4.61 (s, 1H, NH), 4.57 (s, 2H, NHCH_2), 3.86 (s, 2H, SeCH_2), 1.71 (s, 9H, C(CH_3)₃); ^{13}C NMR (75 MHz, CDCl_3) δ 151.69, 146.78, 138.31, 137.09, 131.33, 130.46, 120.15, 117.20, 113.89, 61.43, 40.08, 32.44, 29.63; MS (ESI): m/z = found 502.04 [M^+ + Na]; calcd. 479.02 [M^+]; HRMS calcd. for $\text{C}_{19}\text{H}_{22}\text{BrN}_5\text{Se}$ [M^+ + Na]: 502.01160, found 502.01065 [M^+ + Na]. Anal. Calcd for $\text{C}_{19}\text{H}_{22}\text{BrN}_5\text{Se}$ (479.02): C, 47.61; H, 4.63; N, 14.61. Found: C, 47.63; H, 4.65; N, 14.63.

4.4.7. 4-((4-bromobenzyl)selanyl)-*N*-((1-(*tert*-butyl)-1*H*-tetrazol-5-yl)(4-chlorophenyl)methyl)aniline (**9**)

Compound **9** was prepared following procedure II from 4-((4-bromobenzyl)selanyl)aniline **4c** (341 mg, 1 mmol), 4-chlorobenzaldehyde (155 mg, 1.1 mmol), azidotrimethylsilane (146 μ L, 1.1 mmol) and *tert*-butyl isocyanide (125 μ L, 1.1 mmol). Completion was monitored via TLC ligroin: acetic ester = 4:3, R_f = 0.35, purified using silica gel with ligroin: acetic ester = 3:2. White solid; Yield: 477 mg (81%); mp 181–182 °C. ^1H NMR (300 MHz, CDCl_3) δ 7.30 – 7.25 (m, 2H, Ar-H), 7.22 (dt, J = 5.0, 1.9 Hz, 3H, Ar-H), 7.18 (d, J = 2.5 Hz, 1H, Ar-H), 7.15 – 7.08 (m, 2H, Ar-H), 6.86 – 6.78 (m, 2H, Ar-H), 6.47 – 6.41 (m, 2H, Ar-H), 6.02 (s, 1H, NH), 4.83 (d, J = 9.4 Hz, 1H, CH), 3.81 (s, 2H, SeCH_2), 1.65 (s, 9H, C(CH_3)₃); ^{13}C NMR (75 MHz, CDCl_3) δ 154.62, 145.55, 139.77, 138.33, 137.06, 136.31, 134.82, 131.45, 131.27, 130.46, 129.39, 129.09, 114.69, 62.61, 59.61, 30.16, 29.78; MS (ESI): m/z = found 612.02 [M^+ + Na]; calcd. 589.01 [M^+]; HRMS calcd. for $\text{C}_{25}\text{H}_{25}\text{BrClN}_5\text{Se}$ [M^+ + Na]: 612.00393, found 612.00287 [M^+ + Na]. Anal. Calcd for $\text{C}_{25}\text{H}_{25}\text{BrClN}_5\text{Se}$ (589.01): C, 50.91; H, 4.27; N, 11.87. Found: C, 50.93; H, 4.28; N, 11.88.

4.4.8. 4-((4-bromobenzyl)selanyl)-*N*-((1-(*tert*-butyl)-1*H*-tetrazol-5-yl)(4-methoxyphenyl)methyl)aniline (**10**)

Compound **10** was prepared following procedure II from 4-((4-bromobenzyl)selanyl)aniline **4c** (341 mg, 1 mmol), 4-methoxybenzaldehyde (122 μ L, 1.1 mmol), azidotrimethylsilane (146 μ L, 1.1 mmol) and *tert*-butyl isocyanide (125 μ L, 1.1 mmol). Completion was monitored via TLC ligroin: acetic ester = 4:3, R_f = 0.30, purified using silica gel with ligroin: acetic ester = 3:2. White solid; Yield: 620 mg (86%); mp

152–153 °C. ¹H NMR (300 MHz, CDCl₃) δ 7.23 – 7.20 (m, 1H, Ar-H), 7.18 – 7.08 (m, 4H, Ar-H), 6.85 – 6.77 (m, 5H, Ar-H), 6.47 – 6.40 (m, 2H, Ar-H), 5.98 (s, 1H, NH), 4.80 (d, *J* = 9.2 Hz, 1H, CH), 3.77 (s, 2H, SeCH₂), 3.72 (s, 3H, OCH₃), 1.61 (s, 9H, C(CH₃)₃); ¹³C NMR (75 MHz, CDCl₃) δ 159.86, 155.18, 145.37, 138.44, 137.05, 131.26, 130.46, 129.72, 129.08, 120.30, 117.19, 114.71, 114.56, 61.75, 55.33, 53.89, 32.39, 30.08; MS (ESI): *m/z* = found 607.86 [M⁺ + Na]; calcd. 585.06 [M⁺]; HRMS calcd. for C₂₆H₂₈BrN₅OSe [M⁺ + Na]: 608.05347, found 608.05270 [M⁺ + Na]. Anal. Calcd for C₂₆H₂₈BrN₅OSe (585.06): C, 53.35; H, 4.82; N, 11.96. Found: C, 53.37; H, 4.81; N, 11.95.

4.4.9. *N*-(*tert*-butyl)-2-(*N*-(4-((2,2-diethoxyethyl)selanyl)phenyl)acetamido)acetamide (**11**)

Compound **11** was prepared following procedure I from 4-((2-ethoxy-3-methoxypropyl)selanyl)aniline **4a** (289 mg, 1 mmol), paraformaldehyde (33 mg, 1.1 mmol), acetic acid (63 μL, 1.1 mmol) and *tert*-butyl isocyanide (125 μL, 1.1 mmol). Completion was monitored via TLC ligroin: acetic ester = 4:3, R_f = 0.25, purified using silica gel with ligroin: acetic ester = 3:2. White solid; Yield: 346 mg (78%); mp 113–114 °C. ¹H NMR (300 MHz, CDCl₃) δ 7.55 – 7.40 (m, 2H, Ar-H), 7.13 – 6.99 (m, 2H, Ar-H), 6.00 (s, 1H, NH), 4.66 (t, *J* = 5.6 Hz, 1H, CH), 4.05 (s, 2H, NHCH₂), 3.66 – 3.45 (m, 4H, 2OCH₂), 3.10 (d, *J* = 5.6 Hz, 2H, SeCH₂), 1.85 (s, 3H, CH₃CO), 1.28 (s, 9H, C(CH₃)₃), 1.14 (t, *J* = 7.0 Hz, 6H, 2CH₃); ¹³C NMR (75 MHz, DMSO) δ 169.57, 167.58, 142.62, 132.39, 128.97, 102.08, 61.94, 52.46, 50.61, 30.81, 28.96, 22.59, 15.61; MS (ESI): *m/z* = found 467.21 [M⁺ + Na]; calcd. 444.15 [M⁺]; HRMS calcd. for C₂₀H₃₂N₂O₄Se [M⁺ + Na]: 467.139769, found 467.13978[M⁺ + Na]. Anal. Calcd for C₂₀H₃₂N₂O₄Se (444.15): C, 54.17; H, 7.27; N, 6.32. Found: C, 54.15; H, 7.26; N, 6.31.

4.4.10. *N*-(*tert*-butyl)-2-(4-chlorophenyl)-2-(*N*-(4-((2,2-diethoxyethyl)selanyl)phenyl)acetamido)acetamide (**12**)

Compound **12** was prepared following procedure I from 4-((2-ethoxy-3-methoxypropyl)selanyl)aniline **4a** (289 mg, 1 mmol), 4-chlorobenzaldehyde (155 mg, 1.1 mmol), acetic acid (63 μL, 1.1 mmol) and *tert*-butyl isocyanide (125 μL, 1.1 mmol). Completion was monitored via TLC ligroin: acetic ester = 4:3, R_f = 0.33, purified using silica gel with ligroin: acetic ester = 3:2. White solid; Yield: 415 mg (75%); mp 91–92 °C. ¹H NMR (300 MHz, CDCl₃) δ 7.25 (t, *J* = 10.1 Hz, 2H, Ar-H), 7.08 (d, *J* = 8.5 Hz, 2H, Ar-H), 6.99 (d, *J* = 8.5 Hz, 2H, Ar-H), 6.94 (d, *J* = 23.8 Hz, 2H, Ar-H), 5.93 (s, 1H, NH), 5.61 (s, 1H, CH), 4.58 (t, *J* = 5.6 Hz, 1H, CH), 3.70 – 3.34 (m, 4H, 2OCH₂), 3.04 (d, *J* = 5.6 Hz, 2H, SeCH₂), 1.77 (s, 3H, CH₃CO), 1.29 (s, 9H, C(CH₃)₃), 1.12 (t, *J* = 7.0 Hz, 6H, 2CH₃); ¹³C NMR (75 MHz, CDCl₃) δ 170.10, 167.49, 137.85, 133.42, 132.29, 131.27, 130.68, 130.29, 129.83, 127.54, 101.09, 63.17, 61.12, 50.66, 29.94, 27.63, 22.21, 14.22; MS (ESI): *m/z* = found 577.20 [M⁺ + Na]; calcd. 554.15 [M⁺]; HRMS calcd. for C₂₆H₃₅ClN₂O₄Se [M⁺ + Na]: 577.13428, found 577.13210 [M⁺ + Na]. Anal. Calcd for C₂₆H₃₅ClN₂O₄Se (554.15): C, 56.37; H, 6.37; N, 5.06. Found: C, 56.39; H, 6.38; N, 5.07.

4.4.11. *N*-(*tert*-butyl)-2-(*N*-(4-((2,2-diethoxyethyl)selanyl)phenyl)acetamido)-2-(4-hydroxyphenyl)acetamide (**13**)

Compound **13** was prepared following procedure I from 4-((2-ethoxy-3-methoxypropyl)selanyl)aniline **4a** (289 mg, 1 mmol), 4-hydroxybenzaldehyde (134 mg, 1.1 mmol), acetic acid (63 μL, 1.1 mmol) and *tert*-butyl isocyanide (125 μL, 1.1 mmol). Completion was monitored via TLC ligroin: acetic ester = 4:3, R_f = 0.31, purified using silica gel with ligroin: acetic ester = 3:2. White solid; Yield: 384 mg (65%); mp 98–99 °C. ¹H NMR (300 MHz, CDCl₃) δ 7.25 (d, *J* = 8.4 Hz, 2H, Ar-H), 6.87 (dd, *J* = 10.8, 8.9 Hz, 3H, Ar-H), 6.71 – 6.53 (m, 3H, Ar-H), 5.78 (s, 1H, NH), 5.46 (s, 1H, CH), 4.63 (t, *J* = 5.6 Hz, 1H, CH), 3.67 – 3.40 (m, 4H, 2OCH₂), 3.03 (d, *J* = 5.6 Hz, 2H, SeCH₂), 1.79 (s, 3H, CH₃CO), 1.25 (s, 9H, C(CH₃)₃), 1.13 (t, *J* = 7.0 Hz, 6H, 2CH₃); ¹³C NMR (75 MHz, CDCl₃) δ 171.27, 169.11, 156.50, 139.46, 132.78, 131.67, 130.95, 130.54, 126.07, 115.56, 101.85, 64.93, 62.09, 61.77, 51.61, 31.17, 28.65, 23.25, 15.22, 15.19; MS (ESI): *m/z* = found 559.22 [M⁺ + Na]; calcd. 536.18 [M⁺]; HRMS calcd. for C₂₆H₃₆N₂O₅Se [M⁺ + Na]: 559.16817, found 559.16716[M⁺ + Na]. Anal. Calcd for C₂₆H₃₆N₂O₅Se (536.18): C, 58.31; H, 6.78; N, 5.23. Found: C, 58.33; H, 6.79; N, 5.23.

4.4.12. *N*-(*tert*-butyl)-2-(*N*-(4-((2,2-diethoxyethyl)selanyl)phenyl)acetamido)-2-(4-methoxyphenyl)acetamide (**14**)

Compound **14** was prepared following procedure I from 4-((2-ethoxy-3-methoxypropyl)selanyl)aniline **4a** (289 mg, 1 mmol), 4-methoxybenzaldehyde (122 μL, 1.1 mmol), acetic acid (63 μL, 1.1 mmol) and *tert*-butyl isocyanide (125 μL, 1.1 mmol). Completion was monitored via TLC ligroin: acetic ester = 4:3, R_f = 0.33, purified using silica gel with ligroin: acetic ester = 3:2. White solid; Yield: 423 mg (77%); mp 101–102 °C. ¹H NMR (300 MHz, CDCl₃) δ 7.34 – 7.14 (m, 2H, Ar-H), 7.08 – 6.85 (m, 3H, Ar-H), 6.73 – 6.53 (m, 3H, Ar-H), 5.85 (s, 1H, NH), 5.44 (s, 1H, CH), 4.60 (t, *J* = 5.7 Hz, 1H, CH), 3.75 (s, 3H, OCH₃), 3.63 – 3.38 (m, 4H, 2OCH₂), 3.04 (d, *J* = 5.6 Hz, 2H, SeCH₂), 1.77 (s, 3H, CH₃CO), 1.25 (s, 9H, C(CH₃)₃), 1.11 (t, *J* = 7.0 Hz, 6H, 2CH₃); ¹³C NMR (75 MHz, CDCl₃) δ 169.92, 168.07, 158.47, 138.30, 131.22, 130.60, 129.98, 129.74, 125.78, 112.71, 101.07, 63.41, 61.11, 61.07, 54.14, 50.52, 29.95, 27.66, 22.25, 14.21; MS (ESI): *m/z* = found 573.23 [M⁺ + Na]; calcd. 550.19 [M⁺]; HRMS calcd. for C₂₇H₃₈N₂O₅Se [M⁺ + Na]: 573.18382, found 573.18170[M⁺ + Na]. Anal. Calcd for C₂₇H₃₈N₂O₅Se (550.19): C, 59.01; H, 6.97; N, 5.10. Found: C, 59.03; H, 6.98; N, 5.11.

4.4.13. *N*-(4-((4-bromobenzyl)selanyl)phenyl)-*N*-(2-(*tert*-butylamino)-2-oxoethyl)acetamide (**15**)

Compound **15** was prepared following procedure I from 4-((4-bromobenzyl)selanyl)aniline **4c** (341 mg, 1 mmol), paraformaldehyde (33 mg, 1.1 mmol), acetic acid (63 μL, 1.1 mmol) and *tert*-butyl isocyanide (125 μL, 1.1 mmol). Completion was monitored via TLC ligroin: acetic ester = 4:3, R_f = 0.36, purified using silica gel with ligroin: acetic ester = 1:1. White solid; Yield: 396 mg (80%); mp 144–145 °C. ¹H NMR (300 MHz, CDCl₃) δ 7.39 – 7.33 (m, 2H,

Ar-H), 7.31 – 7.24 (m, 2H, Ar-H), 7.10 – 7.04 (m, 2H, Ar-H), 7.02 – 6.95 (m, 2H, Ar-H), 6.00 (s, 1H, NH), 4.07 (s, d, 2H, CH₂), 4.00 (s, 2H, SeCH₂), 1.85 (s, 3H, CH₃CO), 1.28 (s, 9H, C(CH₃)₃); ¹³C NMR (75 MHz, CDCl₃) δ 171.11, 167.74, 142.70, 137.21, 134.87, 131.56, 130.53, 130.13, 128.17, 120.85, 54.77, 51.32, 31.41, 28.74, 22.34; MS (ESI): *m/z* = found 518.97 [M⁺ + Na]; calcd. 496.03 [M⁺]; HRMS calcd. for C₂₁H₂₅N₂O₂Se [M⁺ + Na]: 519.01568, found 519.01309 [M⁺ + Na]. Anal. Calcd for C₂₁H₂₅N₂O₂Se (496.03): C, 50.82; H, 5.08; N, 5.64. Found: C, 50.80; H, 5.09; N, 5.65.

4.4.14. 2-(*N*-(4-(4-bromobenzyl)selanyl)phenyl)acetamido)-*N*-(*tert*-butyl)-2-(4-chlorophenyl)acetamide (**16**)

Compound **16** was prepared following procedure I from 4-((4-bromobenzyl)selanyl)aniline **4c** (341 mg, 1 mmol), 4-chlorobenzaldehyde (155 mg, 1.1 mmol), acetic acid (63 μL, 1.1 mmol) and *tert*-butyl isocyanide (125 μL, 1.1 mmol). Completion was monitored via TLC ligroin: acetic ester = 4:3, R_f = 0.34, purified using silica gel with ligroin: acetic ester = 3:2. White solid; Yield: 460 mg (76%); mp 129–130 °C. ¹H NMR (300 MHz, CDCl₃) δ 7.42 – 7.23 (m, 2H, Ar-H), 7.21 – 7.13 (m, 2H, Ar-H), 7.12 – 7.05 (m, 2H, Ar-H), 7.03 – 6.96 (m, 2H, Ar-H), 6.93 – 6.87 (m, 4H, Ar-H), 5.87 (s, 1H, NH), 5.57 (s, 1H, CH), 3.95 (s, 2H, SeCH₂), 1.76 (s, 3H, COCH₃), 1.27 (s, 9H, C(CH₃)₃); ¹³C NMR (75 MHz, CDCl₃) δ 169.98, 167.45, 138.61, 136.38, 133.46, 133.16, 132.22, 130.68, 130.48, 129.99, 129.42, 129.07, 127.57, 119.79, 63.05, 50.70, 30.35, 27.63, 22.19; MS (ESI): *m/z* = found 629.03 [M⁺ + Na]; calcd. 606.02 [M⁺]; HRMS calcd. for C₂₇H₂₈BrN₂O₂Se [M⁺ + Na]: 629.00801, found 629.00756 [M⁺ + Na]. Anal. Calcd for C₂₇H₂₈BrN₂O₂Se (606.02): C, 53.44; H, 4.65; N, 4.62. Found: C, 53.46; H, 4.66; N, 4.63.

4.4.15. 2-(*N*-(4-(4-bromobenzyl)selanyl)phenyl)acetamido)-*N*-(*tert*-butyl)-2-(4-methoxyphenyl)acetamide (**17**)

Compound **17** was prepared following procedure I from 4-((4-bromobenzyl)selanyl)aniline **4c** (341 mg, 1 mmol), 4-methoxybenzaldehyde (122 μL, 1.1 mmol), acetic acid (63 μL, 1.1 mmol) and *tert*-butyl isocyanide (125 μL, 1.1 mmol). Completion was monitored via TLC ligroin: acetic ester = 4:3, R_f = 0.35, purified using silica gel with ligroin: acetic ester = 3:2. White solid; Yield: 451 mg (75%); mp 172–173 °C. ¹H NMR (300 MHz, CDCl₃) δ 7.35 – 7.29 (m, 2H, Ar-H), 7.26 – 7.22 (m, 3H), 7.14 (d, *J* = 8.1 Hz, 3H, Ar-H), 6.95 – 6.91 (m, 2H, Ar-H), 6.90 – 6.84 (m, 2H, Ar-H), 6.69 – 6.60 (m, 2H, Ar-H), 5.85 (s, 1H, NH), 5.41 (s, 1H, CH), 3.87 (s, 2H, SeCH₂), 3.69 (s, 3H, OCH₃), 1.76 (s, 3H, COCH₃), 1.26 (s, 9H, C(CH₃)₃); ¹³C NMR (75 MHz, CDCl₃) δ 180.55, 169.98, 158.83, 140.20, 139.21, 138.99, 134.20, 132.82, 131.70, 131.20, 128.02, 120.18, 115.93, 113.74, 90.34, 55.21, 50.68, 30.80, 28.68, 23.64; MS (ESI): *m/z* = found 625.08 [M⁺ + Na]; calcd. 602.07 [M⁺]; HRMS calcd. for C₂₈H₃₁BrN₂O₃Se [M⁺ + Na]: 625.05755, found 625.05648 [M⁺ + Na]. Anal. Calcd for C₂₈H₃₁BrN₂O₃Se (602.07): C, 55.83; H, 5.19; N, 4.65. Found: C, 55.81; H, 5.19; N, 4.66.

4.4.16. (*E*)-2-(4-(4-chlorobenzylidene)amino)phenylselanyl)-3-methylnaphthalene-1,4-dione (**18**)

Compound **18** was synthesized from 2-((4-aminophenyl)selanyl)-3-methylnaphthalene-1,4-dione **4d** (343 mg, 1 mmol) and

4-chlorobenzaldehyde (155 μL, 1.1 mmol) in methanol. Completion was monitored via TLC ligroin: acetic ester = 4:1, R_f = 0.36, purified using silica gel with ligroin: acetic ester = 3:1. Yellow solid; Yield: 418 mg (90%); mp 78–79 °C. ¹H NMR (300 MHz, CDCl₃) δ 8.34 (d, *J* = 9.4 Hz, 1H, N = CH), 8.00 (dd, *J* = 17.3, 8.7 Hz, 2H, Ar-H), 7.79 – 7.71 (m, 2H, Ar-H), 7.67 – 7.56 (m, 2H, Ar-H), 7.53 – 7.46 (m, 2H, Ar-H), 7.41 – 7.34 (m, 2H, Ar-H), 7.07 – 7.01 (m, 2H, Ar-H), 2.16 (s, 3H, CH₃); ¹³C NMR (75 MHz, CDCl₃) δ 182.46, 181.60, 159.32, 151.44, 149.94, 147.05, 134.61, 133.73, 133.55, 132.28, 132.06, 130.04, 129.22, 127.10, 126.91, 126.78, 121.92, 117.87, 115.83, 17.81; MS (ESI): *m/z* = found 488.05 [M⁺ + Na]; calcd. 465.00 [M⁺]; HRMS calcd. for C₂₄H₁₆ClNO₂Se [M⁺ + Na]: 487.99270, found 487.99076 [M⁺ + Na]. Anal. Calcd for C₂₄H₁₆ClNO₂Se (465.00): C, 62.02; H, 3.47; N, 3.01. Found: C, 62.04; H, 3.48; N, 3.02.

4.4.17. (*E*)-2-(4-(4-methoxybenzylidene)amino)phenylselanyl)-3-methylnaphthalene-1,4-dione (**19**)

Compound **19** was synthesized from 2-((4-aminophenyl)selanyl)-3-methylnaphthalene-1,4-dione **4d** (343 mg, 1 mmol) and 4-methoxybenzaldehyde (134 μL, 1.1 mmol) in methanol. Completion was monitored via TLC ligroin: acetic ester = 4:1, R_f = 0.35, purified using silica gel with ligroin: acetic ester = 3:1. Yellow solid; Yield: 406 mg (88%); mp 109–110 °C. ¹H NMR (300 MHz, DMSO) δ 8.48 (s, 1H, N = CH), 8.02 – 7.88 (m, 2H, Ar-H), 7.85 – 7.74 (m, 4H, Ar-H), 7.55 – 7.45 (m, 2H, Ar-H), 7.13 – 7.07 (m, 2H, Ar-H), 7.01 (d, *J* = 8.8 Hz, 2H, Ar-H), 3.78 (s, 3H, OCH₃), 2.07 (s, 3H, CH₃); ¹³C NMR (75 MHz, DMSO) δ 184.32, 182.25, 162.52, 160.81, 150.21, 147.66, 147.71, 145.71, 136.18, 134.59, 133.92, 132.28, 131.04, 127.00, 126.81, 126.76, 122.66, 114.77, 109.51, 55.90, 18.35; MS (ESI): *m/z* = found 462.06 [M⁺ + 1]; calcd. 461.05 [M⁺]; HRMS calcd. for C₂₅H₁₉NO₃Se [M⁺ + Na]: 462.06029, found 462.05924 [M⁺ + H]. Anal. Calcd for C₂₅H₁₉NO₃Se (461.05): C, 65.22; H, 4.16; N, 3.04. Found: C, 65.24; H, 4.15; N, 3.03.

Declaration of Competing Interest

The authors declare that they have no known competing financial interests or personal relationships that could have appeared to influence the work reported in this paper.

Acknowledgments

The author thanks Mansoura University, the Science and Technology Development Fund (Egypt), the Embassy of France (Egypt). The author thanks the Conseil Régional de Bourgogne (France) and the Ministère de l'Enseignement et de la Recherche (France). This article is based upon work from COST Action CA16112-NutRedOx (*Personalized Nutrition in aging society: redox control of major age-related diseases*), supported by COST (European Cooperation in Science and Technology).

Appendix A. Supplementary data

Supplementary data to this article can be found online at <https://doi.org/10.1016/j.arabjc.2021.103051>.

References

- Liu, Y., Zhou, J., 2013. Oligodendrocytes in neurodegenerative diseases. *Front. Biol.* 8, 127–133.
- Hughes, A.N., Appel, B., 2019. Oligodendrocytes express synaptic proteins that modulate myelin sheath formation. *Nat. Commun.* 10, 1–15.
- Bechler, M.E., Byrne, L., 2015. CNS myelin sheath lengths are an intrinsic property of oligodendrocytes. *Curr. Biol.* 25, 2411–2416.
- El Waly, B., Macchi, M., Cayre, M., Durbec, P., 2014. Oligodendrogenesis in the normal and pathological central nervous system. *Front. Neurosci.* 8, 145–166.
- Coman, I., Barbin, G., Charles, P., Zalc, B., Lubetzki, C., 2005. Axonal signals in central nervous system myelination, demyelination and remyelination. *J. Neurol. Sci.* 233, 67–71.
- Vanzulli, I., Papanikolaou, M., La Rocha, De, Irene Chacon, F., Pieropan, A.D., Rivera, D., Gomez-Nicola, A., Verkhratsky, J.J., Rodríguez, A.M Butt, 2020. Disruption of oligodendrocyte progenitor cells is an early sign of pathology in the triple transgenic mouse model of Alzheimer's disease. *Neurobiol. Aging.*
- Ransohoff, R.M., 2016. How neuroinflammation contributes to neurodegeneration. *Science* 353, 777–783.
- Mahalingaiah, P.K., Singh, K.P., 2014. Chronic oxidative stress increases growth and tumorigenic potential of MCF-7 breast cancer cells. *PLoS ONE* 9, e87371.
- Karihtala, P., Kauppila, S., Puistola, U., Jukkola-Vuorinen, A., 2012. Absence of the DNA repair enzyme human 8-oxoguanine glycosylase is associated with an aggressive breast cancer phenotype. *Br. J. Cancer.* 106, 344–347.
- Ibrahim, M., Muhammad, N., Naeem, M., Deobald, A.M., Kamdem, J.P., Rocha, J.B., 2015. In vitro evaluation of glutathione peroxidase (GPx)-like activity and antioxidant properties of an organoselenium compound. *Toxicol. In Vitro.* 29, 947–952.
- Pisoschi, A.M., Pop, A., 2015. The role of antioxidants in the chemistry of oxidative stress. *Eur. J. Med. Chem.* 97, 55–74.
- Meriane, D., Genta-Jouve, G., Kaabeche, M., Michel, S., Boutef-nouchet, S., 2014. Rapid Identification of Antioxidant Compounds of Genista saharae Coss. & Dur. by Combination of DPPH Scavenging Assay and HPTLC-MS. *Molecules* 19, 4369–4379.
- Correa, P., Fonham, E.T., Bravo, J.C., Bravo, L.E., Ruiz, B., Zarama, G., Realpe, J.L., Malcom, G.T., Li, D., Johnson, W.D., 2000. Chemoprevention of gastric dysplasia: randomized trial of antioxidant supplements and anti-Helicobacter pylori therapy. *J. Natl. Cancer Inst.* 92, 1881–1888.
- Pons, D.G., Moran, C., Alorda-Clara, M., Oliver, J., Roca, P., Sastre-Serra, J., 2020. Micronutrients Selenomethionine and Selenocysteine Modulate the Redox Status of MCF-7 Breast Cancer Cells. *Nutrients.* 12, 865–875.
- Haselton, K.J., David, R., Fell, K., Schulte, E., Dybas, M., Olsen, K. W., Kanzok, S.M., 2015. Molecular cloning, characterization and expression profile of a glutathione peroxidase-like thioredoxin peroxidase (TPx) of the rodent malaria parasite *Plasmodium berghei*. *Parasitol. Int.* 64, 282–289.
- Luo, Z., Liang, L., Sheng, J., Pang, Y., Li, J., Huang, L., Li, X., 2014. Synthesis and biological evaluation of a new series of ebsele derivatives as glutathione peroxidase (GPx) mimics and cholinesterase inhibitors against Alzheimer's disease. *Bioorg. Med. Chem.* 22, 1355–1361.
- Parnham, M.J., Sies, H., 2013. The early research and development of ebsele. *Biochem. Pharmacol.* 86, 1248–1253.
- Kreihl, S., Loewinger, M., Florian, S., Kipp, A.P., Banning, A., Wessjohann, L.A., Brauer, M.N., Iori, R., Esworthy, R.S., Chu, F., Brigelius-Flohé, R., 2012. Glutathione peroxidase-2 and selenium decreased inflammation and tumors in a mouse model of inflammation-associated carcinogenesis whereas sulforaphane effects differed with selenium supply. *Carcinogenesis* 33, 620–628.
- Nascimento, V., Alberto, E.E., Tondo, D.W., Dambrowski, D., Detty, M.R., Nome, F., Braga, A.L., 2012. GPx-Like activity of selenides and selenoxides: experimental evidence for the involvement of hydroxy perhydroxy selenane as the active species. *J. Am. Chem. Soc.* 134, 138–141.
- Barbosa, N.V., Nogueira, C.W., Nogara, P.A., de Bem, A.F., Aschner, M., Rocha, J.B., 2017. Organoselenium compounds as mimics of selenoproteins and thiol modifier agents. *Metallomics.* 9, 1703–1734.
- Mugesh, G., du Mont, W.W., Sies, H., 2001. Chemistry of biologically important synthetic organoselenium compounds. *Chem. Rev.* 101, 2125–2179.
- Bhabak, K.P., Mugesh, G., 2010. Functional mimics of glutathione peroxidase: bioinspired synthetic antioxidants. *Acc. Chem. Res.* 43, 1408–1419.
- Moyad, M.A., 2020. Preventing Lethal Prostate Cancer with Diet, Supplements, and Rx: Heart Healthy Continues to Be Prostate Healthy and “First Do No Harm” Part II. *Curr. Urol. Reports.* 21, 1–10.
- Álvarez-Pérez, M., Ali, W., Maré, M.A., Handzlik, J., Domínguez-Álvarez, E., 2018. Selenides and diselenides: a review of their anticancer and chemopreventive activity. *Molecules* 23, 628–646.
- Ali, W., Álvarez-Pérez, M., Maré, M.A., Salardón-Jiménez, N., Handzlik, J., Domínguez-Álvarez, E., 2018. The anticancer and chemopreventive activity of selenocyanate-containing compounds. *Curr. Pharmacol. Reports.* 4, 468–481.
- Yamaguchi, T., Sano, K., Takakura, K., Saito, I., Shinohara, Y., Asano, T., Yasuhara, H., 1998. Ebsele in acute ischemic stroke: a placebo-controlled, double-blind clinical trial. *Stroke* 29, 12–17.
- Dias, G.R., de Almeida, T.M., Sudati, J.H., Dobrachinski, F., Pavin, S., Soares, F.A., Nogueira, C.W., Barbosa, N.B., 2014. Diphenyl diselenide supplemented diet reduces depressive-like behavior in hypothyroid female rats. *Physiol. Behav.* 124, 116–122.
- Glaser, V., Martins Rde, P., Vieira, A.J., Oliveira Ede, M., Straliootto, M.R., Mukdsi, J.H., Torres, A.I., de Bem, A.F., Farina, M., da Rocha, J.B., De Paul, A.L., Latini, A., 2014. Diphenyl diselenide administration enhances cortical mitochondrial number and activity by increasing hemoxygenase type 1 content in a methylmercury-induced neurotoxicity mouse model. *Mol. Cell. Biochem.* 390, 1–8.
- Giordani, C.F., de Souza, D., Dornelles, L., Nogueira, C.W., Alves, M.P., Prigol, M., Rodrigues, O.E., 2014. Diphenyl diselenide-loaded nanocapsules: preparation and biological distribution. *Appl. Biochem. Biotechnol.* 172, 755–766.
- Shaaban, S., Ashmawy, A.M., Negm, A., Wessjohann, L.A., 2019. Synthesis and biochemical studies of novel organic selenides with increased selectivity for hepatocellular carcinoma and breast adenocarcinoma. *Eur. J. Med. Chem.* 179, 515–526.
- Shaaban, S., Negm, A., Ashmawy, A.M., Ahmed, D.M., Wessjohann, L.A., 2016. Combinatorial synthesis, in silico, molecular and biochemical studies of tetrazole-derived organic selenides with increased selectivity against hepatocellular carcinoma. *Eur. J. Med. Chem.* 122, 55–71.
- Cherkaoui-Malki, M., Shaaban, S., Tahri-Joutey, M., Elshobaky, A., Saih, F., Vervandier-Fasseur, D., Jacob, C., Nasser, B., Latruffe, N., Andreoletti, P., 2019. Cytoprotective and Antioxidants in Peroxisomal Neurodegenerative Diseases. *Multidisciplinary Digital Publishing Institute Proceedings.* 11, 33–35.
- Myznikov, L.V., Hrabalek, A., Koldobskii, G.I., 2007. Drugs in the tetrazole series. (Review). *Chem. Heterocycl. Compd.* 43, 1–9.
- Song, W.H., Liu, M.M., Zhong, D.W., Zhu, Y.L., Bosscher, M., Zhou, L., Ye, D.Y., Yuan, Z.H., 2013. Tetrazole and triazole as bioisosters of carboxylic acid: discovery of diketo tetrazoles and diketo triazoles as anti-HCV agents. *Bioorg. Med. Chem. Lett.* 23, 4528–4531.

- Lacerda, R.B., Sales, N.M., da Silva, L.L., Tesch, R., Miranda, A.L., Barreiro, E.J., Fernandes, P.D., Fraga, C.A., 2014. Novel potent imidazo[1,2-a]pyridine-N-Glyciny-hydrazone inhibitors of TNF- α production: in vitro and in vivo studies. *PLoS ONE* 9, e91660.
- Shmatova, O.I., Nenajdenko, V.G., 2013. Synthesis of tetrazole-derived organocatalysts via azido-Ugi reaction with cyclic ketimines. *J. Org. Chem.* 78, 9214–9222.
- Ostrovskii, V.A., Trifonov, R.E., Popova, E.A., 2013. Medicinal chemistry of tetrazoles. *Russ. Chem. Bull.* 61, 768–780.
- Shaaban, S., Negm, A., Sobh, M.A., Wessjohann, L.A., 2016. Expedient Entry to Functionalized Pseudo-peptidic Organoselenide Redox Modulators via Sequential Ugi/SN Methodology. *Anticancer Agents Med. Chem.* 16 (5), 621–632.
- Shaaban, S., Negm, A., Sobh, M.A., Wessjohann, L.A., 2015. Organoselenocyanates and symmetrical diselenides redox modulators: Design, synthesis and biological evaluation. *Eur. J. Med. Chem.* 97, 190–201.
- Rivera, D.G., Vasco, A.V., Echemendía, R., Concepción, O., Pérez, C. S., Gavín, J.A., Wessjohann, L.A., 2014. A Multicomponent Conjugation Strategy to Unique N-Steroidal Peptides: First Evidence of the Steroidal Nucleus as a γ -Turn Inducer in Acyclic Peptides, *Chemistry*?. *Eur. J.* 20, 13150–13161.
- Miller, S. Exploring Avenues in Synthetic Methodology: Novel Approaches to Organoselenium and Organofluorine Chemistry, and Greener Methods for Oxidation and Amidation, (2019). Doctoral Dissertations. 2293.
- Lenardão, E.J., Santi, C., Sancineto, L., 2018. *New Frontiers in Organoselenium Compounds*. Springer.
- Krief, A., Hevesi, L., 2012. *Organoselenium Chemistry I: Functional Group Transformations*. Springer Science & Business Media.
- Edgar, N., Sibille, E., 2012. A putative functional role for oligodendrocytes in mood regulation. *Transl. Psychiatry.* 2, e109.
- Feutz, A.C., Pham-Dinh, D., Allinquant, B., Miehe, M., Ghandour, M.S., 2001. An immortalized jimpy oligodendrocyte cell line: defects in cell cycle and cAMP pathway. *Glia.* 34, 241–252.
- Baarine, M., Ragot, K., Genin, E.C., El Hajj, H., Trompier, D., Andreoletti, P., Ghandour, M.S., Menetrier, F., Cherkaoui-Malki, M., Savary, S., Lizard, G., 2009. Peroxisomal and mitochondrial status of two murine oligodendrocytic cell lines (158N, 158JP): potential models for the study of peroxisomal disorders associated with dysmyelination processes. *J. Neurochem.* 111, 119–131.
- A. Zarrouk, A. Vejux, T. Nury, H. El Hajj I., M. Haddad, M. Cherkaoui-Malki, J. Riedinger, M. Hammami, G. Lizard, Induction of Mitochondrial Changes Associated with Oxidative Stress on Very Long Chain Fatty Acids (C22:0, C24:0, or C26:0)-Treated Human Neuronal Cells (SK-NB-E), *Oxid. Med. Cell. Longev.* 2012 (2012) 623257.
- Vejux, A., Kahn, E., Dumas, D., Bessede, G., Menetrier, F., Athias, A., Riedinger, J.M., Frouin, F., Stoltz, J.F., Ogier-Denis, E., Todd-Pokropek, A., Lizard, G., 2005. 7-Ketocholesterol favors lipid accumulation and colocalizes with Nile Red positive cytoplasmic structures formed during 7-ketocholesterol-induced apoptosis: analysis by flow cytometry, FRET biphoton spectral imaging microscopy, and subcellular fractionation. *Cytometry A.* 64, 87–100.
- Zubair, H., Khan, H.Y., Sohail, A., Azim, S., Ullah, M.F., Ahmad, A., Sarkar, F.H., Hadi, S.M., 2013. Redox cycling of endogenous copper by thymoquinone leads to ROS-mediated DNA breakage and consequent cell death: putative anticancer mechanism of antioxidants. *Cell. Death Dis.* 4, e660.
- Bair, J.S., Palchadhuri, R., Hergenrother, P.J., 2010. Chemistry and biology of deoxyxybenzoquinone, a potent inducer of cancer cell death. *J. Am. Chem. Soc.* 132, 5469–5478.
- Kiran Aithal, B., Sunil Kumar, M.R., Nageshwar Rao, B., Udupa, N., Satish Rao, B.S., 2009. Juglone, a naphthoquinone from walnut, exerts cytotoxic and genotoxic effects against cultured melanoma tumor cells. *Cell Biol. Int.* 33, 1039–1049.
- Shaaban, S., Sasse, F., Burkholz, T., Jacob, C., 2014. Sulfur, selenium and tellurium pseudo-peptides: synthesis and biological evaluation. *Bioorg. Med. Chem.* 22, 3610–3619.
- Xu, J., Gong, Y., Sun, Y., Cai, J., Liu, Q., Bao, J., Yang, J., Zhang, Z., 2020. Impact of selenium deficiency on inflammation, oxidative stress, and phagocytosis in mouse macrophages. *Biol. Trace Elem. Res.* 194, 237–243.
- He, X., Zhong, M., Li, S., Li, X., Li, Y., Li, Z., Gao, Y., Ding, F., Wen, D., Lei, Y., 2020. Synthesis and biological evaluation of organoselenium (NSAIDs-SeCN and SeCF₃) derivatives as potential anticancer agents. *Eur. J. Med. Chem.* 112864.
- Cardoso, B.R., Roberts, B.R., Bush, A.I., Hare, D.J., 2015. Selenium, selenoproteins and neurodegenerative diseases. *Metallomics.* 7, 1213–1228.
- Sharma, A.K., Amin, S., 2013. Post SELECT: selenium on trial. *Future Med. Chem.* 5, 163–174.
- Sanmartin, C., Plano, D., Sharma, A.K., Palop, J.A., 2012. Selenium compounds, apoptosis and other types of cell death: an overview for cancer therapy. *Int. J. Mol. Sci.* 13, 9649–9672.
- Galant, L.S., Rafique, J., Braga, A.L., Braga, F.C., Saba, S., Radi, R., da Rocha, João, Batista Teixeira, C., Santi, M., Monsalve, M. Farina, 2020. The thiol-modifier effects of organoselenium compounds and their cytoprotective actions in neuronal cells. *Neurochem. Res.*, 1–11
- Chen, Z., Lai, H., Hou, L., Chen, T., 2020. Rational design and action mechanisms of chemically innovative organoselenium in cancer therapy. *Chem. Commun.* 56, 179–196.
- Nogueira, C.W., Rocha, J.B., 2011. Toxicology and pharmacology of selenium: emphasis on synthetic organoselenium compounds. *Arch. Toxicol.* 85, 1313–1359.
- Doering, M., Ba, L.A., Lilienthal, N., Nicco, C., Scherer, C., Abbas, M., Zada, A.A., Coriat, R., Burkholz, T., Wessjohann, L., Diederich, M., Batteux, F., Herling, M., Jacob, C., 2010. Synthesis and selective anticancer activity of organochalcogen based redox catalysts. *J. Med. Chem.* 53, 6954–6963.
- Karlsson, M., Kurz, T., Brunk, U.T., Nilsson, S.E., Frennesson, C.I., 2010. What does the commonly used DCF test for oxidative stress really show?. *Biochem. J.* 428, 183–190.
- Nury, T., Zarrouk, A., Vejux, A., Doria, M., Riedinger, J.M., Delage-Mourroux, R., Lizard, G., 2014. Induction of oxiaoptophagy, a mixed mode of cell death associated with oxidative stress, apoptosis and autophagy, on 7-ketocholesterol-treated 158N murine oligodendrocytes: impairment by alpha-tocopherol. *Biochem. Biophys. Res. Commun.* 446, 714–719.
- Luchese, C., Brandao, R., Acker, C.I., Nogueira, C.W., 2012. 2,2'-Dipyridyl Diselenide is a Better Antioxidant than Other Disubstituted Diaryl Diselenides. *Mol. Cell. Biochem.* 367, 153–163.
- Tian, X., Schaich, K.M., 2013. Effects of molecular structure on kinetics and dynamics of the trolox equivalent antioxidant capacity assay with ABTS(+*). *J. Agric. Food Chem.* 61, 5511–5519.
- Mecklenburg, S., Shaaban, S., Ba, L.A., Burkholz, T., Schneider, T., Diesel, B., Kiemer, A.K., Röseler, A., Becker, K., Reichrath, J., Stark, A., Tilgen, W., Abbas, M., Wessjohann, L.A., Sasse, F., Jacob, C., 2009. Exploring synthetic avenues for the effective synthesis of selenium- and tellurium-containing multifunctional redox agents. *Org. Biomol. Chem.* 7, 4753–4762.
- Plano, D., Baquedano, Y., Moreno-Mateos, D., Font, M., Jiménez-Ruiz, A., Palop, J.A., Sanmartin, C., 2011. Selenocyanates and diselenides: A new class of potent antileishmanial agents. *Eur. J. Med. Chem.* 46, 3315–3323.
- Shaaban, S., Diestel, R., Hinkelmann, B., Muthukumar, Y., Verma, R.P., Sasse, F., Jacob, C., 2012. Novel peptidomimetic compounds containing redox active chalcogens and quinones as potential anticancer agents. *Eur. J. Med. Chem.* 58, 192–205.
- Wang, Q., Cui, K., Espin-Garcia, O., Cheng, D., Qiu, X., Chen, Z., Moore, M., Bristow, R.G., Xu, W., Der, S., Liu, G., 2013. Resistance to bleomycin in cancer cell lines is characterized by

- prolonged doubling time, reduced DNA damage and evasion of G2/M arrest and apoptosis. *PLoS ONE* 8, e82363.
- Evans, P.J., Halliwell, B., 1994. Measurement of iron and copper in biological systems: bleomycin and copper-phenanthroline assays. *Methods Enzymol.* 233, 82–92.
- Mira, A., Gimenez, E.M., Bolzan, A.D., Bianchi, M.S., Lopez-Larraz, D.M., 2013. Effect of thiol compounds on bleomycin-induced DNA and chromosome damage in human cells. *Arch. Environ. Occup. Health.* 68, 107–116.
- Straliotto, M.R., de Oliveira, J., Mancini, G., Bainy, A.C., Latini, A., Deobald, A.M., Rocha, J.B., de Bem, A.F., 2013. Disubstituted diaryl diselenides as potential atheroprotective compounds: Involvement of TrxR and GPx-like systems. *Eur. J. Pharm. Sci.* 48, 717–725.
- Mashat, K.H., Babgi, B.A., Hussien, M.A., Arshad, M.N., Abdellatif, M.H., 2019. Synthesis, structures, DNA-binding and anticancer activities of some copper (I)-phosphine complexes. *Polyhedron* 158, 164–172.
- Al-Hazmi, G.A., Abou-Melha, K.S., El-Metwaly, N.M., Althagafi, I., Shaaban, F., Zaky, R., 2020. Green synthesis approach for Fe (III), Cu (II), Zn (II) and Ni (II)-Schiff base complexes, spectral, conformational, MOE-docking and biological studies. *Appl. Organometallic Chem.* 34, e5403.
- Al-Hazmi, G.A., Abou-Melha, K.S., El-Metwaly, N.M., Althagafi, I., Zaki, R., Shaaban, F., 2019. Green Synthesis for 3-(2-Benzoylhydrazono)-N-(pyridin-2-yl) butanamide Complexes: Spectral, Analytical, Modelling, MOE Docking and Biological Studies. *J. Inorg. Organomet. Polym Mater.*, 1–18
- Al-Hazmi, G.A., Abou-Melha, K.S., El-Metwaly, N.M., Althagafi, I., Shaaban, F., Elghalban, M.G., El-Gamil, M.M., 2020. Spectroscopic and theoretical studies on Cr (III), Mn (II) and Cu (II) complexes of hydrazone derived from picolinic hydrazide and O-vanillin and evaluation of biological potency. *Appl. Organomet. Chem.* 34, e5408.
- Althagafi, I., El-Metwaly, N.M., Farghaly, T., 2019. Characterization of new Pt (IV)-thiazole complexes: Analytical, spectral, molecular modeling and molecular docking studies and applications in two opposing pathways. *Appl. Organomet. Chem.* 33, e5099.
- He, H., Zhou, Y., Liang, F., Li, D., Wu, J., Yang, L., Zhou, X., Zhang, X., Cao, X., 2006. Combination of porphyrins and DNA-alkylation agents: synthesis and tumor cell apoptosis induction. *Bioorg. Med. Chem.* 14, 1068–1077.
- Shaaban, S., Gaffer, E.H., Jabar, Y., Elmorsy, S.S., 2015. Cytotoxic naphthalene based-symmetrical diselenides with increased selectivity against MCF-7 breast cancer cells. *Int. J. Pharmacy.* 5, 738–746.
- Shaaban, S., Gaffer, E.H., Alshahd, M., Elmorsy, S.S., 2015. Cytotoxic Symmetrical Thiazolediselenides with Increased Selectivity Against MCF-7 Breast Cancer Cells. *Int. J. Res. Develop. Pharm & Life Sci.* 4, 1654–1668.